CALCULATION OF POTENTIAL DISTRIBUTION ALONG A HIGH VOLTAGE TRANSMISSION LINE INSULATOR CHAIN

by

M.R. IRAVANI

A THESIS
Submitted to the Faculty of Graduate Studies
through the Department of Electrical Engineering
in Partial Fulfillment of the requirements for the
Degree of Master of Science at the
UNIVERSITY OF MANITOBA

Winnipeg, Manitoba, Canada

1981

CALCULATION OF POTENTIAL DISTRIBUTION ALONG A HIGH VOLTAGE TRANSMISSION LINE INSULATOR CHAIN

BY

M.R. IRAVANI

A thesis submitted to the Faculty of Graduate Studies of the University of Manitoba in partial fulfillment of the requirements of the degree of

MASTER OF SCIENCE

ABSTRACT

The electrostatic field problem of a HV transmission line insulator chain is solved. The effect of adjacent objects such as tower, cross arm, ground and line conductors, on the field distribution is taken into account. The voltage distribution across the insulator chain is obtained and the effect of environmental conducting bodies on the voltage distribution is discussed.

To analyse the problem, the integral equations are developed for the field domain that consists of several dielectrics and floating electrodes with unknown potential values. Finally, a combination of the integral equation method and the charge simulation technique is employed to solve the 3-dimensional non-axisymmetric insulator chain field problem. The computer programs are developed in general form and can be used for any 3-dimensional field problem.

ACKNOWLEDGEMENT

The author wishes to express his gratitude to his supervisor Dr. M.R. Raghuveer, for his invaluable counselling, guidance and encouragement.

TABLE OF CONTENTS

CHAPTER I

INTRODUCTION

In recent years the rapidly increasing demand for electric power and vital dependance on its continuity have resulted in maintaining the supply reliability at a high level. The increase in voltage level of electric power transmission lines has generated a set of new reliability considerations for insulation designers. One of these is the proper choice of the type of insulator unit and chain which should provide reliable performance of the line.

The behaviour of the insulator chain under normal and adverse climatic conditions depends on the surface electric stress distribution on the chain. A non-uniform stress distribution leads to significant non-uniform atmospheric pollution deposits. This is especially so in the case of HVDC lines. Due to the unidirectional electric forces of DC lines the airborne contamination is more significant than in the AC case. These forces have been shown to predominate over wind forces, and are not so pronounced in the AC case as the time average electric force is zero. The pollution deposits could cause a drastic reduction in the electric strength of the insulator chain due to the process of contamination flashover. Therefore, from the insulation design point of view, an accurate knowledge of the electric field distribution along the insulator chain is important.

Generally, the electrostatic field evaluation due to an insulator chain, requires the solution of Poisson's equation, while meeting specific boundary conditions. This evaluation can be carried out by

applying:

1. *analytical methods* which yield an exact solution
2. *analog methods* which are experimental in nature

and 3. *numerical methods* which provide approximate solutions.

An exact solution of Poisson's equation can be achieved through integrating the differential equation. This is accomplished sometimes by an obvious separation of variables, or by applying a transformation which makes the variables separable. But in practice, physical systems are so complex that analytical solutions are extremely difficult or in fact impossible. Thus, these methods are restricted to a much simpler class of problems.

Analog methods have been used extensively, employing electrolytic tanks, conducting paper, or resistive networks. But they are inaccurate, inconvenient, and expensive. Analog methods are also limited in their application.

Due to the modern achievements in field theory, numerical mathematics and computer science, numerical field evaluation has become more appealing than other methods. During recent years much work has been carried out to develop different numerical methods and to render them applicable to practical situations. Because of the variety of numerical methods available, care must be taken to choose the proper method which can handle the problem in the best way.

In attempts to solve the H.V. transmission line insulator chain field problem, there are basically three difficulties:

1. Extremely complicated insulator chain shape;
2. Unbounded space in which the field computation should be carried out; and

3. The environmental influence on the stress distribution, such as the effect of tower, cross-arm, conductors, and ground.

The range of computational features that each numerical method presents is wide, and it is unlikely that selection of one method without careful pre-considerations results in a successful field solution. The aim of this work is to select the most appropriate available numerical method based on the relevant literature and develop the necessary computer programs for field evaluation of HV insulator chains in its environment.

In Chapter II a short survey of available numerical methods which have been widely used in the high voltage area is reported. The advantages, limitations and latest developments of each method is considered. The integral equation method is selected for computing the field of the insulator chain. In Chapter III the integral equations for the electric field calculation in multi-dielectric media are developed. In Chapter IV the integral equation method is applied to the potential distribution around a single unit insulator and the 400 kV HVDC line insulator chain. Chapter V discusses the effect of tower, cross-arm, ground and conductors on the field distribution of insulator chain. The conclusions are reported in Chapter VI.

CHAPTER II

A SHORT SURVEY OF NUMERICAL METHODS FOR ELECTROSTATIC FIELD CALCULATION

2.1 Introduction

This chapter is concerned with the calculation of electrostatic potential and fields for realistic engineering problems. Five different methods for numerical field evaluation of high voltage apparatus are discussed and compared. Based on the characteristics of different methods, the integral equation method is suggested for the electrostatic field calculation of the HV transmission line insulator chain.

2.2 Mathematical Problem

The common mathematical problem to be solved is the determination of the electrostatic potential $\phi(\bar{r})$ and the field $\bar{E} = -\nabla\phi$ within a 3-dimensional domain V. In general form, the presence of space charge and materials with different permittivity must be taken into account. In this case the potential satisfies Poisson's equation

$$\nabla \cdot \{\varepsilon(\bar{r}) \cdot \nabla\phi(\bar{r})\} + q(\bar{r}) = 0 \qquad (2.1)$$

where $\varepsilon(\bar{r})$ is the dielectric tensor and $q(\bar{r})$ the space charge density. In many practical cases the dielectric permittivity is a scalar, and space charge density is assumed to be zero. Thus equation (2.1) reduces to Laplace's equation

$$\nabla^2\phi(\bar{r}) = 0 \qquad (2.2)$$

The conditions satisfied by ϕ on the boundary R are either Dirichlet boundary conditions

$$\phi(\bar{r}) = \phi_R(\bar{r}) \quad , \quad \bar{r} \text{ on } R \tag{2.3}$$

or Neumann or derivative boundary conditions

$$\bar{n} \cdot (\varepsilon(\bar{r}) \cdot \nabla\phi(\bar{r})) = q_R(\bar{r}) \tag{2.4}$$

where $\bar{n}$ is the unit normal vector on the boundary, and on each part of R either the potential distribution or the surface charge distribution is specified.

2.3 Summary of Computational Methods

Generally, the available numerical methods for electrostatic field calculation can be classified as:

1. finite difference methods (*FDM*)
2. finite element methods (*FEM*)
3. Monte Carlo techniques (*MCT*)
4. integral equation techniques (*IET*)
5. charge simulation methods (*CSM*)

2.3.1 Finite Difference Method

To apply the finite difference method[1-12] to an interior problem, it is required that the potential or its normal derivative is known as boundary conditions. In the finite difference method the solution consists of the potential values at discrete points regularly spaced over the whole field region. These values are obtained by replacing the partial differential equation describing the field by a set of simplified linear equations connecting the potential value of each point

with the potentials at adjacent points. The solution of field problem reduces to that of a system of simultaneous equations. As the consequence of the finite-difference approximation, a rather closely spaced grid points are required to obtain high accuracy. Thus, due to the large number of resulting equations, it is not practical (or economical) to solve the system of equations using techniques involving determination or elimination methods. As a result, either relaxation or iteration techniques are often used.

Boundary relaxation technique[13-15] enables the finite difference method to be used for two-dimensional or axisymmetric three-dimensional unbounded field problems. This technique temporarily imposes an artifical boundary around region of interest to convert the problem into an interior one. The potential values on this artificial boundary are altered iteratively until they equal exactly those that would be obtained were the infinitely extending mesh problem actually solved. The resulting solution is independent of the choice of artifical boundary.

The main disadvantage of the finite difference method is the difficulty that arises during boundary matching via discrete finite points. This method is not suitable for a medium consisting of several dielectrics, especially when the dielectric-dielectric interfaces and boundary shapes are complicated. This disadvantage can be overcome through application of the finite element method.

2.3.2 Finite Element Method

The finite element method has been frequently used especially in such areas as thermal, mechanical and electrical engineering. This method has been recognized as being the most powerful and versatile technique for field computation. It has also been used in electric field

calculations in high voltage apparatus during recent years[16-19]. The aim of the finite element method is to approximate the actual solution by using a finite number of elements in the entire bounded field region. This can be achieved through establishing a potential approximation function at each surface element and applying the minimum energy principle. It can be shown that the solution of equation (2.1) minimizes the functional[20]

$$F = \frac{1}{2}\int_V \nabla\phi \cdot (\varepsilon(\bar{r}) \cdot \nabla\phi)dv - \int_V q\phi dv - \int_{R'} q_R\phi dR \qquad (2.5)$$

where R' is the part of boundary on which the boundary conditions hold, and F is the total energy of the field within the volume V.

In the finite element method the field domain is divided into M subregions or elements. These elements are usually polyhedra and their edges define a net with N nodes. The function ϕ is to be approximated by a function

$$\psi(\bar{r}) = \sum_{i=1}^{N} f_i(\bar{r})\,\psi_i \qquad (2.6)$$

where f_i are shape functions. Usually each f_i has the following properties:

1. f_i is zero everywhere except within the subregion w_i formed by the elements to which the node i belongs.
2. Across the boundaries of the element w_i, f_i is continuous, and within each element w_i, f_i is a polynomial.

Substituting equation (2.6) in (2.5) gives an approximation F^* to the function F. The minimum of the functional F^* is defined by the conditions

$$\frac{\partial F^*}{\partial \psi_i} = 0 \quad , \quad i = 1, 2, \ldots, N \tag{2.7}$$

The conditions described by (2.7) give a system of linear equation

$$[L]\ [\psi] = [R] \tag{2.8}$$

where $[\psi]$ is the vector of the unknowns and $[R]$ is obtained from the space charge density and boundary conditions described by equations (2.3) and (2.4). The matrix of coefficeints $[L]$ is a square-matrix, positive definite and sparse. The solution of equation (2.8) gives a function ψ which approximates the actual potential ϕ. The field intensity within each element m is given by

$$E_m = (-\nabla\psi)_m = \left(-\sum_{i=1}^{N} \psi_i \nabla f_i\right)_m$$

Often the shape functions f_i's have discontinuous first derivatives. As the maximum size of element tend to zero the computed ψ approaches to the actual solution ϕ, but there are discontinuities in the field intensity at boundaries. For the same field domain discretization more accurate solution can be obtained through employment of shape function that are complete polynomials of higher degrees[21].

The presence of floating electrodes can be allowed by imposing the condition that the potential on the electrode surface, though unknown is constant. For nodes $i, j, k, \ldots$ on this surface

$$\psi_j = \psi_i \quad , \quad \psi_k = \psi_i \quad , \quad \psi_\ell = \psi_i, \ldots.$$

The corresponding equations (2.7) become:

$$\frac{\partial F^*}{\partial \psi_i} + \frac{\partial F^*}{\partial \psi_j} \cdot \frac{\partial \psi_j}{\partial \psi_i} + \frac{\partial F^*}{\partial \psi_k} \cdot \frac{\partial \psi_k}{\partial \psi_i} + \ldots\ldots = 0$$

and matrix L remains symmetric and positive definite.

Variation of dielectric constants within the domain V can also be easily taken into account. The tensor ε which is the functional of equation (2.5) is treated as a function position $\bar{r}$ and considered to be constant within each element. Thus, field problem in the domain consisting several dielectrics and complicated boundary shape can be handled. Generally, implementation of the finite element method requires:

1. Generation of a suitable mesh filling the field domain.
2. Selection of interpolation function, and determination of element properties.
3. Generation of the linear system (2.8) and its solution.
4. Additional computation, if more information is desired.

For two-dimensional geometries, the mesh can be automatically generated; in fact an automatic two-dimensional mesh generator has been developed[22-23]. For three-dimensional problems the mesh must be generated manually, which is a time consuming operation, and usually is an important source of error. For the case of two-dimensional field problems some developments havebeen made that enables the finite element method to be used for exterior field problems[24-26]. Another version of the finite element method for two-dimensional (or three-dimensional axisymmetric) for exterior field problem has been introduced, which combines the charge simulation method with the finite element method[27,28]. It should be mentioned that the main objective of this combination is to use the advantages of both methods to increase the accuracy of solution. Despite the efficient techniques for inversion of sparse matrices, the

finite element and the finite difference methods are not often used for three-dimensional non-axisymmetric geometries, due to the large number of equations to be solved.

2.3.3 Monte Carlo Method

In the Monte Carlo method[29,30] the field region enclosed by the specific boundaries is replaced by a mesh, and the differential equation (2.1) is replaced by the difference equations relating the values of potential at adjacent points of the mesh. The coefficients in the difference equations are interpreted as being the probabilities of transition of a particle from one point to a neighbouring point. This transition is based on the fixed random-walk method[1]. The method which is based on floating random-walk technique[31] is more efficient than the fixed random-walk method. Application of the Monte Carlo method to Laplace's equation is based on the fact that the solution to Laplace's equation, also satisfies the steady-state diffusion equation[32]. For a Laplacian potential $\phi(\bar{r}_0)$ at point $\bar{r}_0$ within the field domain, a series of random walks is constrained according to the following rules:

1. Each walk starts at $\bar{r}_0$.
2. The length of the next step for a walk that reaches a point $\bar{r}$ is equal to the distance between $\bar{r}$ and the nearest point on the boundary.
3. The direction of each step at each walk is chosen at random.
4. Each walk terminates when it approaches within some prearranged small distance from the boundary, the nearest

point on the boundary then being $\bar{r}^*$.

It is found that the average

$$\phi(\bar{r}_0) = \frac{1}{n} \sum_j \phi(\bar{r}_j^*) \tag{2.10}$$

is a statistical estimate of the required $\phi(\bar{r}_0)$ that converges to the correct value as the number of random walks n increases.

As was the case for the finite element and finite difference methods, it is assumed that the region is bounded. However, there are methods which can be used to apply Monte Carlo techniques to unbounded field problems[33]. The most interesting characteristics of the Monte Carlo methods is that the potential can be computed one point at a time. Neither a large array of potentials need to be stored in a computer nor a large number of simultaneous equations need to be solved. In spite of these advantages over the finite element and finite difference methods, this method has not often been used for one- and two-dimensional field problems. In fact, this method requires a considerable time for calculating the potential at each point. The Monte Carlo method is appealing for field solution in the subregion of three-dimensional geometries; it has been shown that as the number of dimensions increase to three, comparative computation favours the Monte Carlo method. This method is not able to handle field problems when floating electrodes with unknown potential values are present.

2.3.4 Integral Equation Technique

Of different numerical methods for solving field problems, the finite element method has been proved to be the most popular one, largely because of its relative ease of application. This method has been very

extensively described in the literature in connection with the bounded field problems with prescribed boundary conditions. However, there are many field problems in which the region of interest occurs outside a defined boundary and extends to infinity, such as the electrostatic field distribution around a high voltage transmission line insulator chain. Several attempts have been made to reduce the problem to a finite size so that it may be readily handled on a digital computer. There include imposition of artificial boundaries that do not exist. Or applying improved versions of the finite element method or the finite difference method for unbounded problems which were mentioned eearlier. The practical difficulties which arise have led to an increasing interest in the integral equation method[34-36]. In this method the material parts of the device are suitably divided and treated as field sources whose magnitudes are to be computed by solving the corresponding integral equations.

By means of Green's Theorem, the Poisson's equation (2.1) in the volume V can be expressed in terms of a volume integral plus a surface integral over the surface, which bounds the volume V.

$$\phi(\bar{X}) = \frac{1}{4\pi\varepsilon} \int_V \frac{q}{r}\, dv + \frac{1}{4\pi} \int_S [\frac{1}{r} \frac{\partial \phi}{\partial n} - \phi \frac{\partial}{\partial n} (\frac{1}{r})]dS \qquad (2.11)$$

where $\phi(\bar{X})$ is the potential at point $\bar{X}$, q is the volume charge density and $\bar{n}$ is the unit vector normal to the surface S. In the case of Laplacian potential, the first integral on the right-hand side is zero. Some additional manipulation yields an expression for the electric potential which is a surface integral over unknown charges. The integral equation is obtained by setting the integral equal to the known potential value of the conductor. The integral equation can then be solved for

the surface charges by approximating the integral as a sum over small surface elements with specific charge distribution. The sum is set equal to the known potential at the center of each surface element. The result of this discretization process is a set of linear algebraic equations which can be solved by standard techniques which is a case of the moment method[37]. Once the charge densities are computed the potential and/or field vector at any point can be determined.

The integral equation method is appealing because it is not necessary to compute the potential at points where it is not desired. Also, the analysis of the problems which are unbounded does not require additional programming effort which the case for the finite element and the finite difference methods. Another distinctive characteristic of integral equa . formulation is that since the unknowns are surface quantities, the number of unknowns will be proportional to the surface area of the region. Thus, for two-dimensional problems, the number of equations is proportional to the permeter of the finite boundary. It follows that the matrix equation obtained through discretizing the integral equation will be of small dimension compared to the matrices obtained for the finite difference and the finite element methods. It appears that the computation time for solutions based on the integral equations will be smaller. Although this conclusion is probably true, it should be recognized that the matrix obtained by the integral equation is dense. As a result, sparse matrix solution techniques[38] useful for accelerating the solution of matrices which can be obtained through application of the finite element and difference methods can not be used. Thus, the computation time advantage due to small matrix size may not be as much as anticipated. It should be noted that efforts have been made to accelerate

the solution of integral equations, constructing matrices larger in dimension but more sparse[39].

Through application of the integral equation method, field problems in the medium of several dielectrics can be solved. For such problems two sets of equations should be derived. One set of equations results from the condition that the potential must be equal to the known potential values on conductor surfaces. The second set of equations results from the fact that the normal component of the flux density at the dielectric-dielectric interfaces must be continuous. If floating electrodes with unknown potential values are present, one additional condition is required. In this case the total charge on each floating electrode with unknown potential should be known. Often this charge value is zero. In the next Chapter this method will be described in detail.

2.3.5 Charge Simulation Method

The charge simulation method[40] consists of replacing the surface charges of each electrode by a set of discrete inner charge distribution, whose positions and type are predetermined, but the magnitudes are unknown. The important point is that if some classical charge distribution *i.e.*, ring, line or point charges are chosen, potential and field vector at any point can be expressed in analytical forms. In the case of Laplacian potential the field vector and potential are given by

$$\phi(\bar{r}) = \sum_j p_j(\bar{r})\, q_j \tag{2.12}$$

$$\bar{E}(\bar{r}) = -\nabla\phi(\bar{r}) = -\sum_j \{\nabla p_j(\bar{r})\} q_j \tag{2.13}$$

where q_j represents the unknown magnitude of the charge on the jth

distribution, and $p_j(\bar{r})$ is a coefficient that depends on the type of distribution and the position of field point $\bar{r}$. The presence of space charge distribution is represented by a set of charges q_k giving additional terms

$$\sum_k p_k(\bar{r})\, q_k$$

and

$$-\sum_k \{\nabla p_k(\bar{r})\} q_k$$

to equations (2.12) and (2.13), respectively.

The potential defined by equation (2.12) satisfies Laplace's equation everywhere in the field domain. Boundary conditions are imposed at a set of collocation points $\bar{r}_i$ on the electrode surfaces. The number of collocation points on each electrode surface is equal to the number of simulating charges. These conditions lead to a system of linear simultaneous equations

$$[p]\,[q] = [\phi] \tag{2.14}$$

where $[p]$ is the matrix of coefficients, $[q]$ is the column matrix of unknown charges and $[\phi]$ is the column matrix of known potential values at collocation points.

The matrix equation (2.14) can be solved employing standard techniques and as the result charge values are obtained. Determining the value of charges, the potential and/or field vector can be computed at any point. When floating electrodes with unknown potential values are present, the matrix equation (2.14) is modified to include the supplementary condition that the sum of simulating charges of each floating electrode must be equal to zero

$$\sum_{j} q_j = 0 \tag{2.15}$$

The simultaneous solution of equations (2.14) and (2.15) gives the value of the unknown charges. When the medium consists of several dielectrics, the polarization charge distribution of each dielectric at the dielectric-dielectric interfaces is substituted by ficticious simulating charges outside the dielectric. Supplementary conditions expressing the continuity of the potential and specifying the discontinuity in normal field component must be satisfied on each interface between two dielectrics. If D_1 and D_2 are two adjacent dielectrics with scalar permittivities ε_1 and ε_2

$$\sum_{q_{j1}} p_j(\bar{r}_i)q_j = \sum_{q_{j2}} p_j(\bar{r}_i)q_j \tag{2.16}$$

$$\varepsilon_1 \sum_{q_{j1}} \bar{n} \cdot \nabla p_j(\bar{r}_i)q_j = \varepsilon_2 \sum_{q_{j2}} \bar{n} \cdot \nabla p_j(\bar{r}_i)q_j \tag{2.17}$$

where q_{j1} consists all charges except those located inside D_1, and q_{j2} consists of charges except those inside D_2. Recently, efforts have been concentrated on developing this method for various geometries and different types of simulation[41-47]. The significant advantage of charge simulation method over other numerical field calculation methods is the relative ease of programming. The disadvantage of this method is that the location of the charges are difficult to determine analytically. Therefore, the accuracy of solution is difficult to predict and depends on personal experience. To some degree this difficulty can be overcome, applying an optimized charge simulation method[48], which determines the position of charges in such a way that the simulation error is minimum.

The charge simulation method has been widely used for the solution of two- and three-dimensional problems. Compared to the integral equation method, to achieve similar accuracy, the charge simulation method requires a larger number of linear equations.

It should be mentioned that for some large and complex geometries it may not be possible to obtain satisfactory solution using only one method. In such cases a fair combination of the foregoing methods may be helpful: *i.e.*, the Monte Carlo method or the charge simulation method can be used to derive a first approximation followed by the finite element method within some reduced subregion of interest. The choice of computational method depends on the problem to be solved according to the criteria set out in Table (2.1).

2.4 Selection of Method for Insulator Chain

The electrostatic field problem of a single unit insulator is an unbounded, three-dimensional axisymmetric problem, which must be solved in a medium of two dielectrics. Due to the complexity of the insulator geometry, application of the finite difference method or the charge simulation method is not convenient. Also, the Monte Carlo method is not applicable, because the field problem is unbounded. The integral equation method or the improved version of the finite element method for unbounded problems can be used to obtain the required field information. These two methods can also be employed for the field evaluation of the insulator chain regardless of the environmental effect on the field distribution. But, due to the large size of the insulator chain, the dimension of the matrix of coefficients increases[5], thus, some difficulties may arise regarding the computer memory and computation time. For the

field calculation of the H.V. transmission insulator chain, when the effect of adjacent conducting bodies are to be considered, the field is an unbounded, three-dimensional and non-symmetric one. In this case the only method which can be applied is the integral equation method.

TABLE 2.1: Comparison of numerical methods for electric field problems

	FEM	FDM	CSM	IET	MCM
Space charge	YES	YES	YES	YES	NO
Floating electrodes	YES	YES	YES	YES	NO
Multi-dielectric medium	YES	Difficult	YES	YES	NO
Extend of solution	Whole domain	Whole domain	Whole domain	Whole domain	Subdomain
Complex boundaries	YES	Difficult	Difficult	YES	YES
Thin electrode field	YES	YES	NO	YES	YES
Surface field	YES	YES	YES	YES	Difficult
Required input data	Large	Large	Small	Small	Small
Computing resources	Large	Large	Small	Small	Small
Exterior problems	YES	YES	YES	YES	NO

CHAPTER III

FIELD CALCULATION FROM THE CHARGE DISTRIBUTION

3.1 Introduction

In this chapter a general solution of Poisson's equation in integral form is obtained by employing Green's theorem. A pair of coupled integral equations are described which can be used to solve for the electric Laplacian potential and field vector. These integral equations can be used for the field calculation in a medium composed of a conducting region with known surface potential and two dielectric regions with scalar permittivities. Lastly, the relations are expanded for obtaining the field solution in a medium composed of several dielectrics and conducting bodies that some of them could be floating electrodes with unknown potential values.

3.2 Integration of Poisson's Equation[55]

By means of Green's theorem (Appendix 1) the potential at a fixed point $\bar{X}$ within a volume V can be expressed in terms of a volume integral plus a surface integral over an arbitrary but regular surface S which encloses volume V, Fig. 3.1. The charge is supposed to be distributed with a volume density of $q(\bar{Y})$. The charge distribution is assumed to be bounded but is an arbitrary function of position. It is not necessary that the surface S encloses all the charge or even any of it,. let 0 be an arbitrary origin and $\bar{X}$ a fixed point of observation within V. The potential at this point due to the entire charge distribution is $\phi(\bar{X})$. A function ψ is chosen in such a way so as to

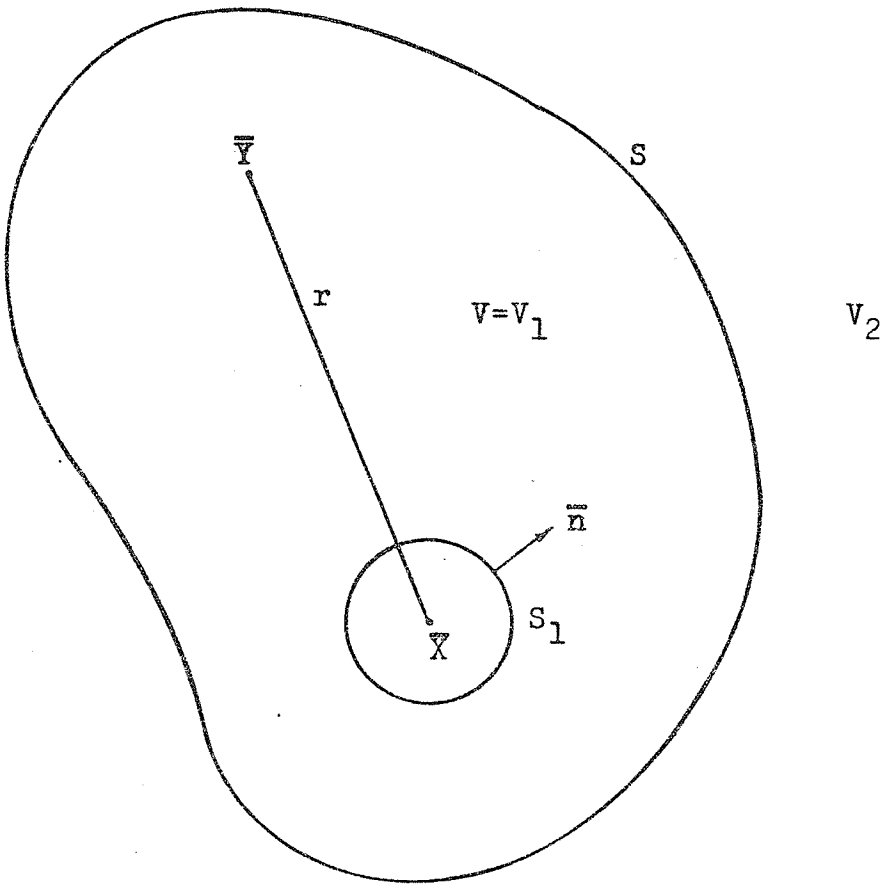

Fig. 3.1 - Application Of Green's Theorem To Region V .

be a spherically symmetrical solution of Laplace's equation

$$\psi(\bar{X}, \bar{Y}) = \frac{1}{r} \tag{3.1}$$

where r is the distance from a variable point $\bar{Y}$ within V to the fixed point $\bar{X}$

$$r = [(x - x')^2 + (y - y')^2 + (z - z')^2]^{\frac{1}{2}}$$

This function however fails to satisfy the necessary conditions of continuity at $r = 0$. To exclude this singularity, a small sphere of radius r_1 is circumscribed about $\bar{X}$ as a center. Then, the volume V is bounded externally by S and internally by S_1. Within V both ϕ and ψ satisfy the requirements of Green's theorem, furthermore because ψ is the solution of Laplace's equation $\nabla^2\psi = 0$. As the result, Green's second identity (Appendix 1) can be reduced to

$$\int_V \frac{1}{r} \nabla^2\phi \, dv = \int_{S+S_1} [\frac{1}{r} \frac{\partial\phi}{\partial n} - \phi \frac{\partial}{\partial n} (\frac{1}{r})] ds \tag{3.2}$$

As shown, the surface integral should be extended over S and S_1. Over the surface S_1 the positive normal direction is directed radially outward from the volume enclosed by S_1. Since this is toward volume V, over S_1 we have

$$\frac{\partial\phi}{\partial n} = \frac{\partial\phi}{\partial r}$$

and $$[\frac{\partial}{\partial n} (\frac{1}{r})] = -\frac{1}{r_1^2} \quad \text{at} \quad r = r_1$$

Since r_1 is constant the contribution of the sphere to the right hand side of (3.2) is

$$\frac{1}{r_1}\int_{S_1}\frac{\partial\phi}{\partial r}\,ds + \frac{1}{r_1^2}\int_{S_1}\phi\,ds$$

If $\bar{\phi}$ and $\partial\bar{\phi}/\partial r$ denote mean values of ϕ and $\partial\phi/\partial r$ on S_1 this contribution is

$$\frac{1}{r_1}\,4\pi r_1^2\,(\partial\bar{\phi}/\partial r) + \frac{1}{r_1^2}\,4\pi r_1^2\,\bar{\phi}$$

and in the limit where r_1 approaches zero reduces to $4\pi\phi(\bar{X})$. Substituting this limiting value in (3.2), the potential at point $\bar{X}$ in the volume V is

$$\phi(\bar{X}) = +\frac{1}{4\pi}\int_V \frac{1}{r}\nabla^2\phi\,dv + \frac{1}{4\pi}\int_S [-\frac{1}{r}\frac{\partial\phi}{\partial n} + \phi\frac{\partial}{\partial n}(\frac{1}{r})]ds \qquad (3.3)$$

When the medium is homogeneous $\nabla^2\phi = -q/\varepsilon$

$$\phi(\bar{X}) = -\frac{1}{4\pi\varepsilon}\int_V \frac{q}{r}\,dv + \frac{1}{4\pi}\int_S [-\frac{1}{r}\frac{\partial\phi}{\partial n} + \phi\frac{\partial}{\partial n}(\frac{1}{r})]ds \qquad (3.4)$$

When the region V bounded by S contains no volume charge

$$\phi(\bar{X}) = \frac{1}{4\pi}\int_S [-\frac{1}{r}\frac{\partial\phi}{\partial n} + \phi\frac{\partial}{\partial n}(\frac{1}{r})]ds \qquad (3.5)$$

It is apparent that the surface integrals in equations(3.4) and (3.5) represent the contribution to the potential at $\bar{X}$ of all charges which are exterior to S. If the values of ϕ and its normal derivatives over S are known, the potential at any interior point can be determined by integration. Equation (3.5) can be interpreted as being a solution to Laplace's equation within V satisfying specific conditions over the boundary. The integral

$$\phi(\bar{X}) = \frac{1}{4\pi\epsilon}\int_V \frac{q}{r}\,dv$$

is a particular solution of Poisson's equation valid at $\bar{X}$, the general solution can be obtained by adding the equation (3.5) to the solution of the homogeneous equation $\nabla^2\phi = 0$. If there are no charges exterior to S, the surface integral must vanish.

3.3 Derivation of Integral Equations

Figure 3.2 shows the problem to be investigated. Region 1 shows the electrode with known potential, regions 2 and 3 indicate two homogeneous dielectrics with scalar permittivities ϵ_2 and ϵ_3, respectively. Thus, the only contributing charges in the potential calculation are the free charges on the electrode surface and polarization charges on dielectric-dielectric interfaces. If this is not the case, then the effect of volume charges must be taken into account[49]. In Fig. 3.2 $\bar{n}_i$ is the unit vector normal to the boundary surface S_i of the volume V_i ($S_i = S_{ij} + S_{ik}$). The potential ϕ_i of the ith region satisfies Laplace's equation

$$\nabla^2\phi_i(\bar{X}) = 0 \tag{3.6}$$

The solution to equation (3.6) in each region is unique subject to the boundary conditions listed below

$$\phi_1 = \phi_2 = \phi_{1S} \quad \text{on } S_{12} \text{ (known)} \tag{3.7}$$

$$\phi_1 = \phi_3 = \phi_{1S} \quad \text{on } S_{13} \text{ (known)} \tag{3.8}$$

$$\phi_2 = \phi_3 \quad \text{on } S_{23} \tag{3.9}$$

$$\phi_3 = 0 \quad \text{at infinity} \tag{3.10}$$

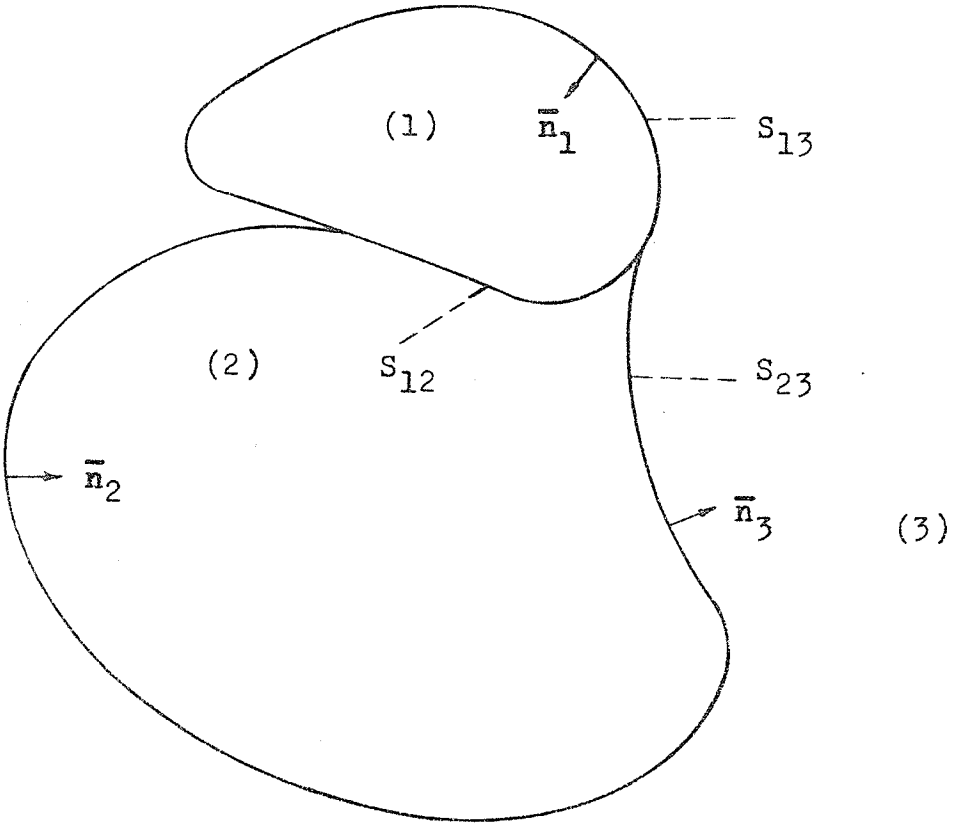

Fig. 3.2 - (1) Conductor

(2) Dielectric ϵ_2

(3) Dielectric ϵ_3

$$\partial\phi_1/\partial n_1 = 0 \qquad \text{on } S_1 \text{ (conducting surface)} \tag{3.11}$$

and

$$\varepsilon_2 \nabla\phi_2 \cdot \bar{n}_2 = -\varepsilon_3 \nabla\phi_3 \cdot \bar{n}_3 \qquad \text{on } S_{23} \tag{3.12}$$

To solve equation (3.6), first, a function $\psi(\bar{X}, \bar{Y})$ is introduced

$$\psi(\bar{X}, \bar{Y}) = 1/(4\pi|\bar{X} - \bar{Y}|)$$

where $\bar{X}$ and $\bar{Y}$ represent field point and source point locations, respectively. Applying Green's theorem for medium V_i

$$\int_{S_i} [-\psi(\bar{X},\bar{Y}) \cdot \partial\phi_i(\bar{Y})/\partial n_i + \phi_i(\bar{Y}) \cdot \partial\psi(\bar{X},\bar{Y})/\partial n_i]ds_i$$

$$= \begin{cases} \phi_i(\bar{X}) & ; \quad \bar{X} \quad \text{in } V_i \\ 0 & ; \quad \bar{X} \quad \text{out of } V_i \end{cases} \tag{3.13}$$

Now applying (3.13) for each region and adding the results, while imposing boundary condition (3.7) to (3.12)

$$\int_{S_{12}} \psi(\bar{X},\bar{Y}) \cdot \partial\phi_2(\bar{Y})/\partial n_1 \, ds$$

$$+ \int_{S_{13}} \psi(\bar{X},\bar{Y}) \cdot \partial\phi_3(Y)/\partial n_1 \, ds$$

$$- (1 - \frac{\varepsilon_3}{\varepsilon_2}) \int_{S_{23}} \psi(\bar{X},\bar{Y}) \partial\phi_3 \, (Y)/\partial n_3 \, ds$$

$$= \begin{cases} \phi_1(\bar{X}) & ; \quad \bar{X} \quad \text{in } V_1 \\ \phi_2(\bar{X}) & ; \quad \bar{X} \quad \text{in } V_2 \\ \phi_3(\bar{X}) & ; \quad \bar{X} \quad \text{in } V_3 \end{cases} \tag{3.14}$$

The terms $(\partial\phi_2/\partial n_1)$ and $(\partial\phi_3/\partial n_1)$ on S_1 and the term $-(1 - \frac{\varepsilon_3}{\varepsilon_2})(\partial\phi_3/\partial n_3)$ on S_{23} can be interpreted as the relative free charge on the conductor-dielectric surface and relative polarization charge on the dielectric-dielectric interface, respectively. Thus, the potential can be recognized to be equal to a summation over all free and polarization charges across interfaces. As it was assumed, since each dielectric is homogeneous, there is no volume polarization charge.

The second equation relating the variables of equation (3.14) can be found by applying the boundary condition given in equation (3.12), across the dielectric-dielectric interface S_{23}. The electric field $\bar{E}_i(\bar{X})$ in any region i can be obtained from equation (3.13)

$$\bar{E}_i(\bar{X}) = -\nabla_x \phi_i(\bar{X}) \tag{3.15}$$

$$= -\int_{S_{12}} \nabla_x\psi(\bar{X},\bar{Y}) \cdot \partial\phi_2(\bar{Y})/\partial n_1 \cdot ds$$

$$-\int_{S_{13}} \nabla_x\psi(\bar{X},\bar{Y}) \cdot \partial\phi_3(\bar{Y})/\partial n_1 \cdot ds$$

$$+ (1 - \frac{\varepsilon_3}{\varepsilon_2}) \int_{S_{23}} \nabla_x\psi(\bar{X},\bar{Y}) \cdot \partial\phi_3(\bar{Y})/\partial n_3 \cdot ds$$

where subscript x indicates that derivatives are taken with respect to the field point $\bar{X}$ coordinates. Inserting equation (3.15) in the boundary condition (3.12), which implies that the normal displacement vector at dielectric interfaces is continuous

$$-(\varepsilon_2 - \varepsilon_3) \int_{S_{12}} (\partial\phi_2(\bar{Y})/\partial n_1) \cdot \nabla_x\psi(\bar{X},\bar{Y})\Big|_{\bar{X}=\bar{P}} \cdot \bar{n}_3 ds$$

$$-(\varepsilon_2 - \varepsilon_3) \int_{S_{13}} (\partial\phi_3(\bar{Y})/\partial n_1) \cdot \nabla_x \psi(\bar{X},\bar{Y})\Big|_{\bar{X}=\bar{P}} \cdot \bar{n}_3 \, ds$$

$$+(\varepsilon_2 - \varepsilon_3) \lim_{\bar{X}_2 = \bar{P}} \int_{S_{23}} (\partial\phi_3(\bar{Y})/\partial n_3) \cdot \nabla_x \psi(\bar{X},\bar{Y}) \cdot \bar{n}_3 \, ds$$

$$-\varepsilon_3(1 - \varepsilon_3/\varepsilon_2) \lim_{\bar{X}_3 = \bar{P}} \int_{S_{23}} (\partial\phi_3(\bar{Y})/\partial n_3) \cdot \nabla_x \psi(\bar{X},\bar{Y}) \cdot \bar{n}_3 \cdot ds = 0 \tag{3.16}$$

where $\bar{P}$ is on the surface S_{23}.

If the charge distribution on a surface S is continuous the normal derivates of the potential generated by the charge distribution at $\bar{X}$ approaches a limit as $\bar{X}$ approaches point $\bar{P}$ on the surface, along the line normal to S from either side[50]. In equation (3.16) the limits

$$\bar{X}_2 = \bar{P} \quad \text{and} \quad \bar{X}_3 = \bar{P}$$

indicate that point field $\bar{X}$ approaches to the boundary S_{23} from mediums 2 and 3, respectively. These two limits for surface S_{23} are as shown below

$$\lim_{\bar{X}_2 = \bar{P}} \int_{S_{23}} (\partial\phi_3(\bar{Y})/\partial n_3) \cdot \nabla_x \psi(\bar{X},\bar{Y}) \cdot \bar{n}_3 \cdot ds$$

$$= \frac{1}{2} (\partial\phi_3(\bar{P})/\partial n_3) + \int_{S_{23}} (\partial\phi_3(\bar{Y})/\partial n_3) \cdot \nabla_x \psi(\bar{X},\bar{Y})\Big|_{\bar{X}=\bar{P}} \cdot \bar{n}_3 \cdot ds$$

$$\lim_{\bar{X}_3 = \bar{P}} \int_{S_{23}} (\partial\phi_3(\bar{Y})/\partial n_3) \cdot \nabla_x \psi(\bar{X},\bar{Y}) \cdot \bar{n}_3 \cdot ds$$

$$= -\frac{1}{2} (\partial\phi_3(\bar{P})/\partial n_3) + \int_{S_{23}} (\partial\phi_3(\bar{Y})/\partial n_3) \cdot \nabla_x \psi(\bar{X},\bar{Y})\Big|_{\bar{X}=\bar{P}} \cdot \bar{n}_3 \cdot ds$$

Substituting the limits in (3.16)

$$-\left(\frac{\varepsilon_2+\varepsilon_3}{2\varepsilon_2}\right)\left(\partial\phi_3(\bar{P})/\partial n_3\right) - \left(1-\frac{\varepsilon_3}{\varepsilon_2}\right)\int_{S_{23}} \left(\partial\phi_3(\bar{Y})/\partial n_3\right) \cdot \left(\partial\psi(\bar{X},\bar{Y})/\partial n_3\right)ds$$

$$+\int_{S_{12}} \left(\partial\phi_2(\bar{Y})/\partial n_1\right) \cdot \left(\partial\psi(\bar{X},\bar{Y})/\partial n_3\right)ds$$

$$+\int_{S_{13}} \left(\partial\phi_3(\bar{Y})/\partial n_1\right) \cdot \left(\partial\psi(\bar{X},\bar{Y})/\partial n_3\right)ds = 0 \qquad (3.17)$$

where $\partial\psi(\bar{X},\bar{Y})/\partial n_3 = \nabla_x\psi(\bar{X},\bar{Y})\Big|_{\bar{X}=\bar{P}} \cdot n_3$

Two coupled integral equations can be achieved by

1. Choosing the field point $\bar{X}$ in equation (3.14) at the electrode surface $S_1 = S_{12} + S_{13}$ and imposing the potential to be equal to the known electrode potential at point $\bar{X}$.
2. Imposing the continuity of normal displacement vector across the dielectric interface S_{23}, employing equation (3.17).

In both equations the unknowns are the charge values $q(\bar{Y})$ which can be defined as

$$q(\bar{Y}) = \partial\phi_2(\bar{Y})/\partial n_1 \quad , \bar{Y} \text{ on } S_{12}$$

$$q(\bar{Y}) = \partial\phi_3(\bar{Y})/\partial n_1 \quad , \bar{Y} \text{ on } S_{13}$$

$$q(\bar{Y}) = -(1-\varepsilon_3/\varepsilon_2)\left(\partial\phi_3(\bar{Y})/\partial n_3\right) \quad , \bar{Y} \text{ on } S_{23}$$

Finally, the integral equations can be written as

$$\phi(\bar{P}) = \int_S q(\bar{Y}) \cdot \psi(\bar{P},\bar{Y})ds \quad , \quad \bar{P} \text{ on } S_1 \tag{3.18}$$

$$(\varepsilon_2+\varepsilon_3)\, q(\bar{P}) = 2(\varepsilon_2-\varepsilon_3) \int_S q(\bar{Y}) \cdot (\partial\psi(\bar{P},\bar{Y})/\partial n_3)ds \quad , \quad \bar{P} \text{ on } S_{23} \tag{3.19}$$

where $S = S_{12} + S_{13} + S_{23}$

$\phi(\bar{P})$ is the known surface potential on S_1

3.4 Extension for More Complex Field Domains

Figure 3.3 illustrates a practical configuration of a medium composed of several dielectrics and electrodes with known potential[28]. The extension of equations (3.18) and (3.19) for such a field domain is straightforward. In such a case, S_1 is the collection of all surfaces over metallic bodies

$$S_1 = (S_{13} + S_{14} + S_{15}) + (S_{23} + S_{24} + S_{25} + S_{26})$$

and S_{23} becomes the collection of all dielectric-dielectric interfaces

$$S_{23} = S_{34} + S_{45} + S_{56}$$

and $S = S_1 + S_{23}$

It should be noted that the application of (3.19) requires the appropriate pair of dielectric constants to be used for any interface.

Figure 3.4 shows a part of HV transmission line insulator chain. Field evaluation around this chain is to be carried out in a medium of two dielectrics and several electrodes. All but two of these electrodes as shown in Fig. 3.4 are floating electrodes with unknown potential values. Application of the integral equation method for the field computation

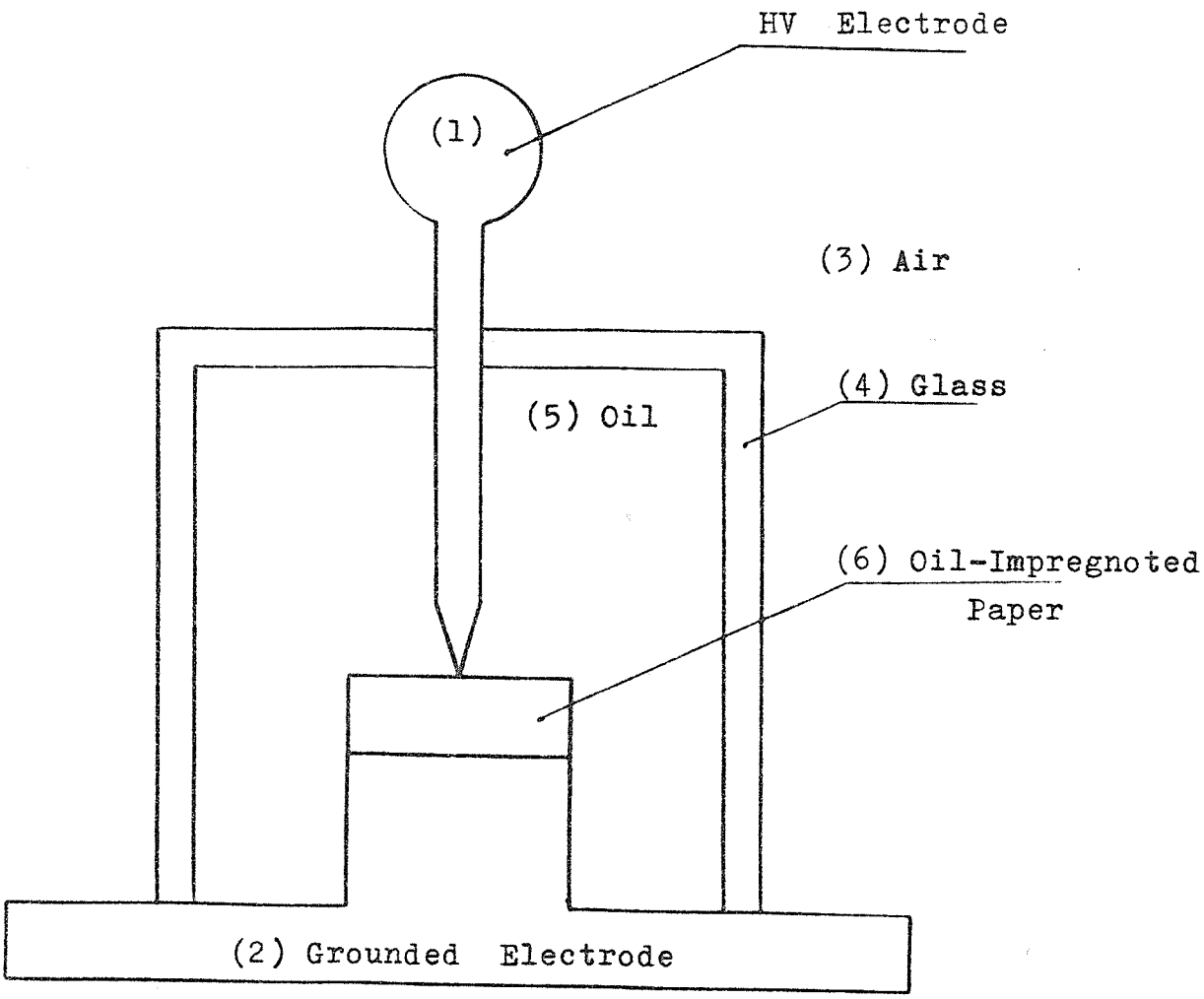

Fig. 3.3 - Field Domain Consisting Of
Several Dielectrics .

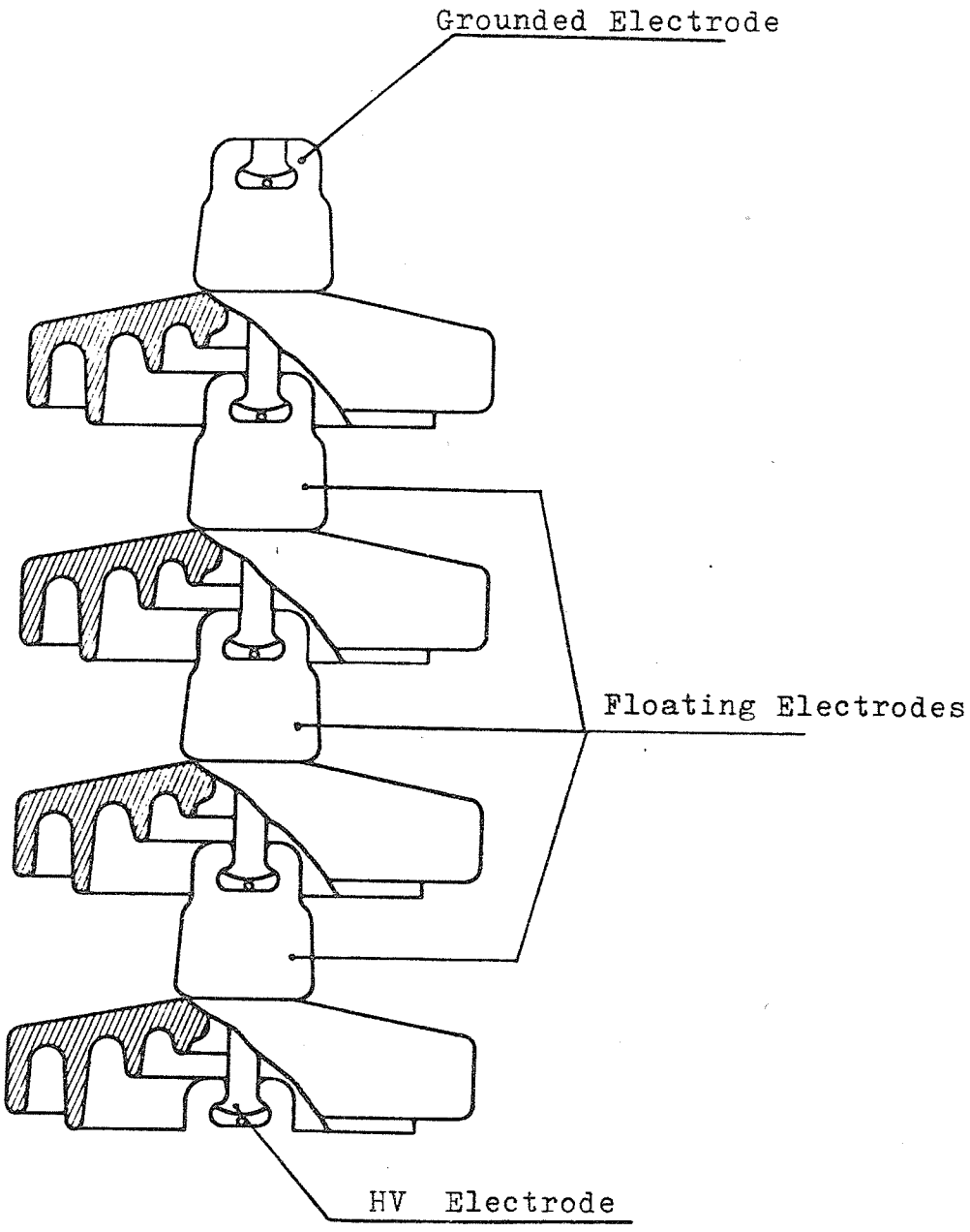

Fig. 3.4 - Field Domain Consisting Of Two Dielectrics And Floating Electrodes .

of such problems requires an additional boundary condition besides the boundary conditions (3.7) to (3.12). In this case the total charge on each floating electrode must be equal to a specific value; often this charge value is zero

$$Q_i = \int_{S_i} q(\bar{Y})\, ds = 0 \qquad (3.20)$$

where S_i is the total surface of floating electrode i.

If the field domain consists of one dielectric, equation (3.19) will be eliminated, which implies that

$$q(\bar{P}) = 0 \quad , \quad \bar{P} \text{ on } S_{23}$$

The application of integral equation in this case reduces to equation (3.18)

$$\phi(\bar{P}) = \frac{1}{\varepsilon} \int_S q(\bar{Y})\, \psi(\bar{P},\bar{Y})\, ds \qquad (3.21)$$

where $\bar{P}$ is on the electrode surface. The above equation can also be derived from superposition of distributed sources.

CHAPTER IV

APPLICATION OF THE INTEGRAL EQUATION METHOD FOR THE ELECTROSTATIC FIELD DISTRIBUTION OF AN INSULATOR CHAIN

4.1 Introduction

In this chapter the integral equations 3.18 and 3.19 are further developed for three-dimensional axisymmetric field problems. The application of the moment method for solving the integral equations is described. The criteria which must be met by the results in order to guarantee the required accuracy are established. The equipotential lines around a single unit insulator are plotted and the effect of different parameters and approximation on the results are discussed. Finally, the field problem of insulator chains composed of 6 and 21 single unit insulators are solved. The potential distribution across the chains are calculated and equipotential lines are illustrated.

4.2 Theoretical Aspects

Before proceeding with the discussion of the equations, the procedures involved in application of the technique for an axisymmetric problem will be described:

1. All the surfaces of the problem under study will be subdivided into a number of axially symmetric subsurfaces.
2. On the subdivisions the free and polarization charge densities will be assumed constant, but of unknown magnitude. Thus, the integral equations 3.18 and 3.19 which

were described earlier can be approximated by a summation. Each term of the summation can be expressed as a constant which is a function of the problem geometry and electrical properties of the dielectrics multiplied by the corresponding unknown charge density.

3. The general form of each term for any axisymmetric problem can be obtained as an analytical expression, but the numerical values are found through application of numerical methods. In the application of the integral equation method to the insulator chain field problem, each subsurface is assumed to have a constant slope. This approximation is equivalent to considering each subsurface ΔS_n to be the lateral surface of a frustum of a cone, as shown in Fig. 4.1. In Fig. 4.1 ℓ is the parametric variable defining the straight-line approximating the contour with each segment lying between ℓ_{n-1} and ℓ_n.

4. A linear system of equations can be obtained by setting equations 3.18 equal to the known potential at the center of each subsurface, on metallic parts, and requiring that equations 3.19 be satisfied at the center of each subsurface on dielectric interfaces.

Hereafter the cylindrical system of coordinates are used and the position of the field point is represented as

$$\bar{X} = (r, z, \theta)$$

and the position of source point is given by

$$\bar{Y} = (r', z', \theta')$$

The surface element ds on each subsurface can be written as

$$ds = r \cdot d\theta' \cdot d\ell$$

where ℓ is the distance along each surface measured from its bottom (Fig. 4.1). r is the cylindrical coordinate perpendicular to the axis of symmetry. For any contour segment, the slope is constant, so ℓ and r can be described as linear functions of z.

$$\begin{aligned} d\ell &= f(z)\, dz \\ r &= r(z) \\ ds &= r(z) \cdot f(z) \cdot d\theta' \cdot dz \end{aligned} \tag{4.1}$$

The separation distance R between the field point $\bar{X}$ and source point $\bar{Y}$ is

$$\begin{aligned} R &= |\bar{X} - \bar{Y}| \\ &= [(r\cos\theta - r'\cos\theta')^2 + (r\sin\theta - r'\sin\theta')^2 + (z - z')^2]^{\frac{1}{2}} \end{aligned} \tag{4.2}$$

In the case of axisymmetric problems, due to angular symmetry, θ can be set equal to zero. So, without loss of generality R may be expressed as:

$$R = [(r - r'\cos\theta')^2 + (r'\sin\theta')^2 + (z - z')^2]^{\frac{1}{2}} \tag{4.3}$$

Furthermore, $q(\bar{Y})$ is a function of z

$$q(\bar{Y}) = q(z) \tag{4.4}$$

Substituting equations (4.1), (4.3) and (4.4) in the integral equations

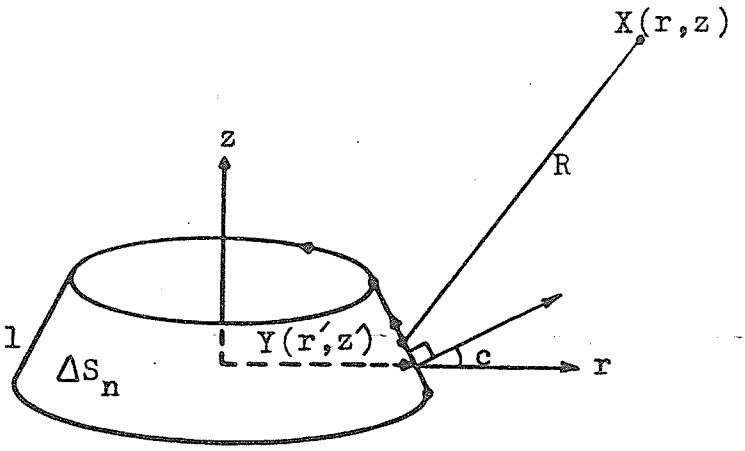

Fig. 4.1- Subsection S_n (Lateral Surface Of Frustum Of Cone).

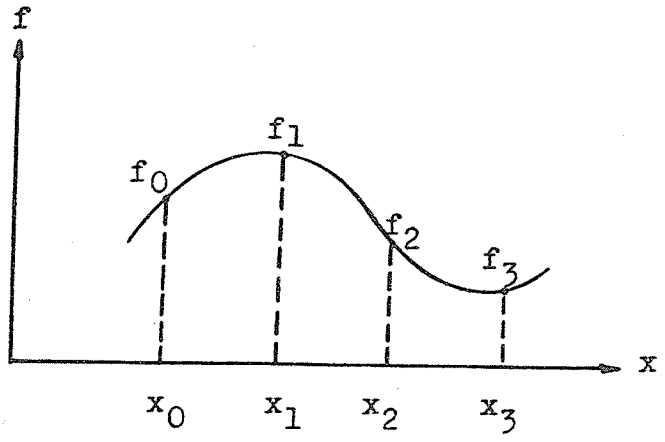

Fig. 4.2- Three-Eights Rule For Numerical Integration.

(3.18) and (3.19) we have

$$\phi(r,z) = \frac{1}{4\pi} \int_{z'} \int_{\theta'} [q(z') \cdot r'(z') \cdot f(z')/R] d\theta' \cdot dz' \qquad (4.5)$$

where r and z are on metallic surfaces.

$$((\varepsilon_2 + \varepsilon_3)/2) \cdot q(r,z) = ((\varepsilon_3 - \varepsilon_2)/4\pi) \int_{z'} \int_{\theta'} q(z') \cdot r'(z') \cdot f(z') \cdot \frac{\partial}{\partial n_3} [1/R] \cdot d\theta' \cdot dz' \qquad (4.6)$$

where r, z are on the dielectric interface.

In both equations (4.5) and (4.6) θ' varies from 0 to 2π, and z' is over each surface in the collection surface taken in succession. In equation (4.5) the term $\int_0^{2\pi} \frac{d\theta'}{R}$ can be expressed as (Appendix 2)

$$G(r,r', z,z') = \int_0^{2\pi} \frac{d\theta'}{R} = \frac{4}{[(r+r')^2 + (z-z')^2]^{\frac{1}{2}}} K(s)$$

where K(s) is the complete integral of the first kind, and

$$S^2 = (4rr')/[(r + r')^2 + (z - z')^2]$$

In equation (4.6) $\frac{\partial}{\partial n_3} \int_0^{2\pi} d\theta'/R$ can be expressed as[51]:

$$\frac{\partial}{\partial n_3} \int_0^{2\pi} d\theta'/R = \frac{\cos(c)}{2r} \left[\frac{[(r')^2 + r^2 + (z-z')^2] E(s) - B^2 K(s)}{AB^2}\right] - \left[\frac{z - z'}{AB^2} \cdot \sin(c)\right]$$

where E(s) is the complete elliptic integral of the second kind.

$$A = [(r + r')^2 + (z - z')^2]^{\frac{1}{2}}$$

$$B = [(r - r')^2 + (z - z')^2]^{\frac{1}{2}}$$

angle C is shown in Fig. 4.1.

Numerical values of K(s) and E(s) can be found by

1. Application of subroutines available in the International Mathematical and Statistical Library (IMSL),

or

2. Employing a polynomial approximation of K(s) and E(s) (Appendix 2). In this case, the approximation can be achieved within 3×10^{-5} or 2×10^{-8} depending on the approximating polynomial.

It should be noted that the analytical expression of the derivatives in equation (4.6) described as

$$\frac{\partial}{\partial n_3} \int_0^{2\pi} \frac{d\theta'}{R} = \nabla\left[\int_0^{2\pi} d\theta'/R\right] \cdot \bar{n}_3$$

can be obtained by finding the derivatives of the polynomial expression of the integral.

4.3 Moment Method for the Solution of the Integral Equations

A procedure which reduces an original functional equation to a matrix equation is called matrix method. The name method of moments has been given to the procedures for obtaining the matrix equation. Sometimes, the procedures is called approximation technique, but when the solution converges in the limit this is a misnomer. Consider the deterministic equation

$$L(q) = v$$

where L is a linear operator, y is known and q is to be determined. Let q be expanded in a series of functions $q_1, q_2, q_3, \ldots$ in the domain of L as

$$q = \Sigma\, c_n\, q_n \tag{4.7}$$

where c_n's are constants. For exact solution the above relation is an infinite summation. For a linear operator L the equation can be written as

$$\sum_n c_n \cdot L\,(q_n) = v \tag{4.8}$$

It is assumed that a suitable inner product $< q, v >$ has been determined. Defining a set of weighting functions $w_1, w_2, w_3, \ldots$ and taking the inner product of equation (4.8) the result is

$$[L_{mn}]\,[q_n] = [V_m]$$

For a nonsingular matrix $[L]$ its inverse exists, and the unknown $[q]$ can be determined. Usually the integration involves in evaluating the elements of coefficients matrix $[L]$ is difficult to perform in problems of practical interest. A simple and effective way to obtain the approximate solution is to require that equation (4.7) be satisfied at the discrete points in the region of interest. This procedure is called point matching method. In terms of the moment method it is equivalent to use the Dirac delta function as a weighting function. For a more accurate solution, other techniques such as the subsectional bases method, the extended operators method, the approximate operators method and perturbation solutions may be applied[52].

4.4 Single Unit Insulator Field Calculation

The whole surface of insulator unit S is divided into N subsurfaces so that each of them is the lateral surface of a cone frustum, designated as ΔS_n (Fig. 4.1).

$$N = N_{1,2} + N_{1,3} + N_{2,3}$$

where $N_{1,3}$ is the number of subsurfaces across metallic part (Pin + Cap) and dielectric ε_2 (glass) interface

$N_{1,3}$ is the number of subsurfaces across metallic part and dielectric ε_1 (air) interface.

$N_{2,3}$ is the number of subsurfaces at the dielectrics interface.

$$S_{1,2} = \sum_n \Delta S_n, \qquad 1 \leq n \leq N_{1,2}$$

$$S_{1,3} = \sum_n \Delta S_n, \qquad N_{1,2} + 1 \leq n \leq N_{1,2} + N_{1,3}$$

and

$$S_{2,3} = \sum_n \Delta S_n, \qquad N_{1,2} + N_{1,3} + 1 \leq n \leq N$$

The surface charge density is approximated as

$$q(z) = \sum_n Q_n \cdot h_n(z) \quad , \quad 1 \leq n \leq N \tag{4.9}$$

where $h_n(z)$ is defined as

$$h_n(z) = \begin{cases} 1 \; ; & z \text{ on } \Delta S_n \\ 0 \; ; & z \text{ on } \Delta S_m \quad , \quad m \neq n \end{cases} \tag{4.10}$$

The charge representation as in equation (4.9) with $h_n(z)$ is defined as (4.10), introduces a charge discontinuity at the boundary of each subsurface. As a result, both the potential value and field vector are

undefined at the lines of discontinuity. However, the expansion function (4.10) is not the only choice, *i.e.*, triangular charge expansion function can be used as an alternative. This would cause additional programming but would result in a continuous function for the surface charge distribution. It is shown that for engineering problems, expansion function (4.10) results in acceptable accuracy[34, 35].

Considering the foregoing discussions equations (4.5) and (4.1) can be written as:

$$\phi(r,z) = \frac{1}{4\pi} \sum_n Q_n \int_{\Delta z'_n} r' \cdot f(z') \cdot G(r,r', z,z') \cdot dz' \quad (4.11)$$

where $1 \leq n \leq N$ and field point (r,z) is on the metallic surfaces

$$Q(r,z) = ((\varepsilon_3 - \varepsilon_2)/(\varepsilon_3 + \varepsilon_2)) \cdot \frac{1}{2\pi} \sum_n Q_n \int_{\Delta z'_n} r' \cdot f(z') \cdot \frac{\partial}{\partial n_3} G(r,r', z,z')dz' \quad (4.12)$$

where $1 \leq n \leq N$ and field point is on the dielectric-dielectric interface.

A system of linear algebraic equations for the unknown Q_n can be obtained, imposing (4.11) to be equal to the known electrode potential at the center of each subsurface on metallic parts, and satisfying (4.12) at the center of each subsurface across dielectrics interface. The total number of unknowns is N which corresponds to $N_{1,2} + N_{1,3}$ on the electrode surfaces and $N_{2,3}$ on dielectrics interface. Representing the coefficient of charges in equations (4.11) and (4.12) by L_{mn}, the equation can be written as:

$$\phi_m = \sum_n L_{mn} Q_n \quad (4.13)$$

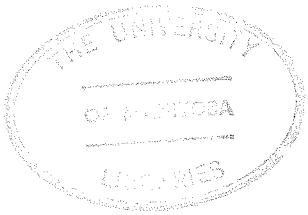

where $1 \leq n \leq N$

$1 \leq m \leq N_{1,2} + N_{1,3}$

$$L_{mn} = \frac{1}{4\pi} \int_{\Delta z'_n} r' \cdot f(z') \cdot G \cdot dz' \tag{4.14}$$

and $$Q_m = \sum_n L_{mn} Q_n \tag{4.15}$$

where $1 \leq n \leq N$

$N_{1,2} + N_{1,3} + 1 \leq m \leq N$

$$L_{mn} = ((\varepsilon_3 - \varepsilon_2)/2\pi \cdot (\varepsilon_3 + \varepsilon_2)) \int_{\Delta z'_n} r' \cdot f(z') \cdot (\partial G/\partial n_3) \cdot dz' \tag{4.16}$$

Equations (4.13) and (4.15) give the matrix equation

$$[L]\ [Q] = [\phi] \tag{4.17}$$

where $[\phi]$ is the column matrix of surface potentials and zeros.

$[Q]$ is the column matrix of unknown surface charge densities.

$[L]$ is the matrix of coefficients.

Determining the unknown charge densities the potential and field vector at any point can be computed. Potential values at any point can be obtained by employing equation (4.13). The field vector can be calculated by:

$$\bar{E} = - \nabla\phi$$

$$\bar{E} = - \sum_n Q_n \cdot \nabla(L_{mn}) \tag{4.18}$$

where

$$\nabla(L_{mn}) = \frac{1}{4\pi} \int_{\Delta z'_n} r' \cdot f(z') \cdot \nabla G \cdot dz' \qquad (4.19)$$

The numerical values of coefficient given by equations (4.14), (4.16) and (4.19) can be found through application of numerical integration methods[53]. The common numerical integration methods for engineering application are trapezoidal rule, Simpson's rule, three-eight rule, and Weddle's rule. It has been experienced Simpson's rule is sufficiently accurate for most engineering purposes. In this work three-eight rule that gives higher precision than Simpson's rule is used. This technique introduces a cubic through the points (x_0, f_0), ..., (x_3, f_3) Fig. 4.2 and the integral is given by

$$\int_{x_0}^{x_3} f(x) \cdot dx \approx \frac{3}{8} h(f_0 + 3f_1 + 3f_2 + f_3)$$

This method is exact for cubical polynomials and has the advantage that it can be applied to an odd number of subintervals.

4.5 Accuracy Criteria

In the integral equation method the accuracy of the results depends on the number of subsurfaces that approximate the actual surface and the position of the subsurfaces. Therefore, some criteria must be established to decide whether the obtained results for each set of surface approximations meet the desired accuracy or not. The following condition can be used as accuracy criteria:

1. The calculated potential on conductors should be equal to the known conductor potential. In other words, the solution must introduce the metallic surfaces as equipotential surfaces.

2. The electric field vector is normal to the electrode surface. As the result the tangential component of the electric field vector at point on electrodes must be equal to zero.

3. The tangential component of the electric field should be continuous across any dielectric-dielectric interface. This condition is the same as the equality of potential values across the interface of two dielectrics, when potentials are calculated respect to each dielectric.

4. The normal component of the displacement vector is continuous across the dielectric-dielectric boundary.

5. The value of electric potential and the field value and direction at any interested point should be independent of the surface approximation.

The conditions 1 to 4 are boundary conditions. The condition 5 is a check which indicates whether the surface approximation is valid.

4.6 Discussion on the Results of Single Insulator Unit

The system of linear equations (4.17) obtained through application of the integral equation method, was used for the electrostatic field calculation of the single unit insulator shown in Fig. 4.3. The field domain consists of two electrodes (Pin and Cap) and two dielectrics (air and glass). The potential values of the Pin and Cap are assumed to be 1 and 0 per unit. The relative permittivities of the glass part and air are 5.5 and 1, respectively. The insulator surface was divided into cone frustum subsurfaces as described earlier. The number of surface segments were changed in the range from 20 to 45 and the system of linear equation (4.17) was solved. For any set of calculated

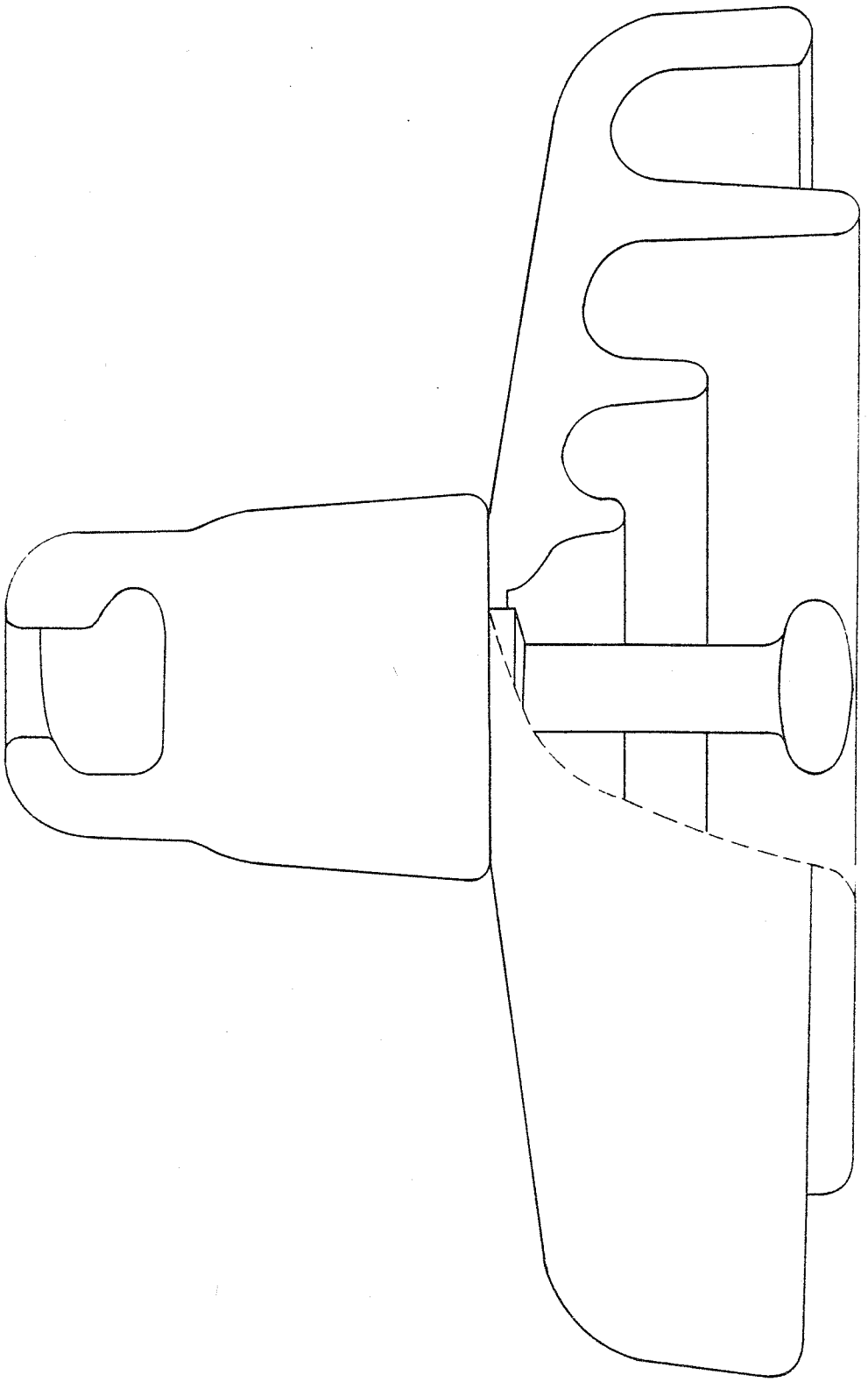

Fig. 4.3- Insulator Unit (168X508 mm).

surface charge values the accuracy criteria 1 to 5 were checked. The results indicate that the best approximation for the single unit insulator can be achieved, employing 30 or 31 subsurfaces as shown in Fig. (4.4a) and (4.4b), respectively. The number of subsurfaces across each part of the insulator unit are:

- 7 subsurfaces on the cap,
- 6 subsurfaces on the pin,
- 17 and 18 subdivisions across the dielectrics interface for Figs. (4.4a) and (4.4b), respectively.

Table 4.1 shows the maximum percent potential error, maximum deviation angle and the maximum percent error of the normal displacement vector for the surface approximation shown in Figs.(4.3a) and (4.4b), where

- Percent potential error = |calculated potential - actual potential| x 100 / (actual potential)
- The deviation angle is the angle between calculated field vector and the normal line to the electrode surface.
- Percent error of the normal displacement vector $\bar{D}$ = |Calculated normal $\bar{D}$ in glass - Calculated normal $\bar{D}$ in air| x 100 / |Calculated normal $\bar{D}$ in glass.

Due to the complexity of the insulator geometry, the boundary can not be expressed in simple algebraic equations. Thus, the digitizer tablet of *PDP-11* was used to generate the coordinates of the check points. The check points are distributed across the boundary with a density of 10 points per unit length in order to check the accuracy criteria mentioned in (4.5). (The digitizer tablet of *PDP-11* is an analog-to-digital converter device, which generates and transfers the x,y coordinates from a drawing to an input computer medium. For the purpose of this work the coordinates were stored in a magnetic tape and

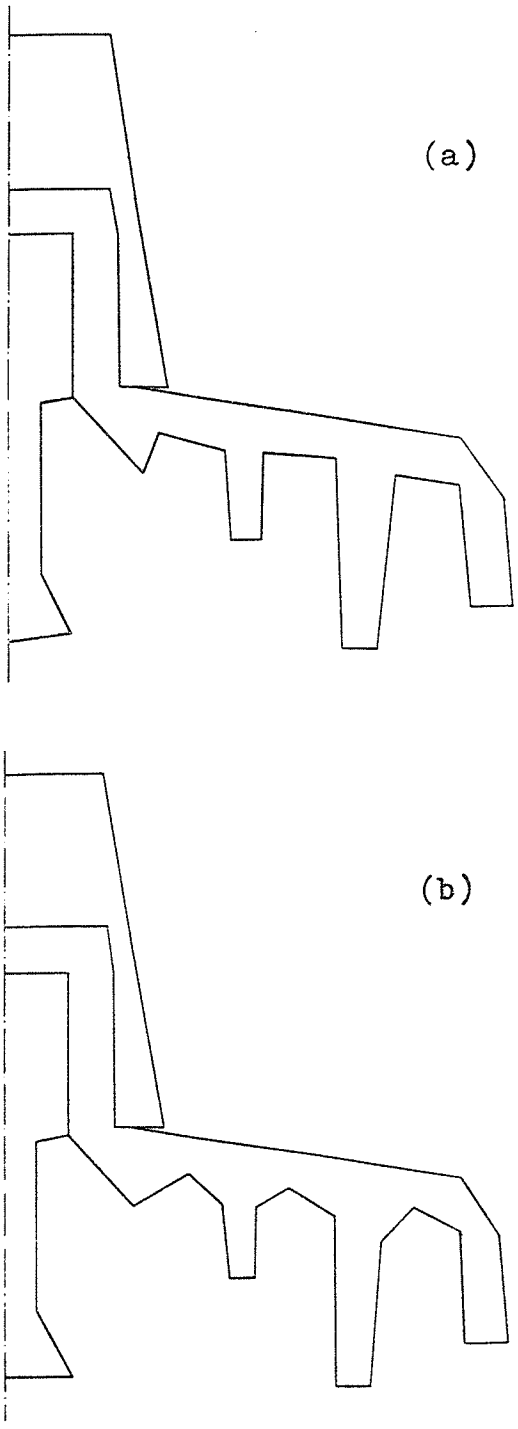

Fig. 4.4- Surface Approximation Of An Insulator Unit With Straight Lines.

then transfered to the main program.) The equipotential lines for the single insulator unit that is approximated as Fig. (4.4b) are shown in Fig. (4.5).

The computer program is developed in general form and can be used for the field calculation of any axisymmetric problem with known electrode potentials in the medium of two dielectrics. Subroutine *LEQT1F* was used for the solution of matrix equation (4.17). Subroutine *SMOCON* was used to plot equipotential lines.

4.7 Field Calculation of the H.V. Insulator Chains

The electrostatic field calculation of a H.V. insulator chain by means of the integral equation method follows the same procedures as described for a single unit insulator, except that the presence of the floating electrodes must be considered. Thus the matrix equation (4.17) will consist of the following equations

$$\phi_m = \sum_n L_{mn} Q_n \qquad (4.13)$$

where - $1 \leq n \leq N$

- $1 \leq m \leq N1$

- N1 is the total number of subsurfaces on the electrodes with known potential values (N11), plus the electrodes with unknown potential values (N12). L_{mn} is given by equation (4.14)

$$Q_m = \sum_n L_{mn} Q_n \qquad (4.15)$$

where - $1 \leq n \leq N$

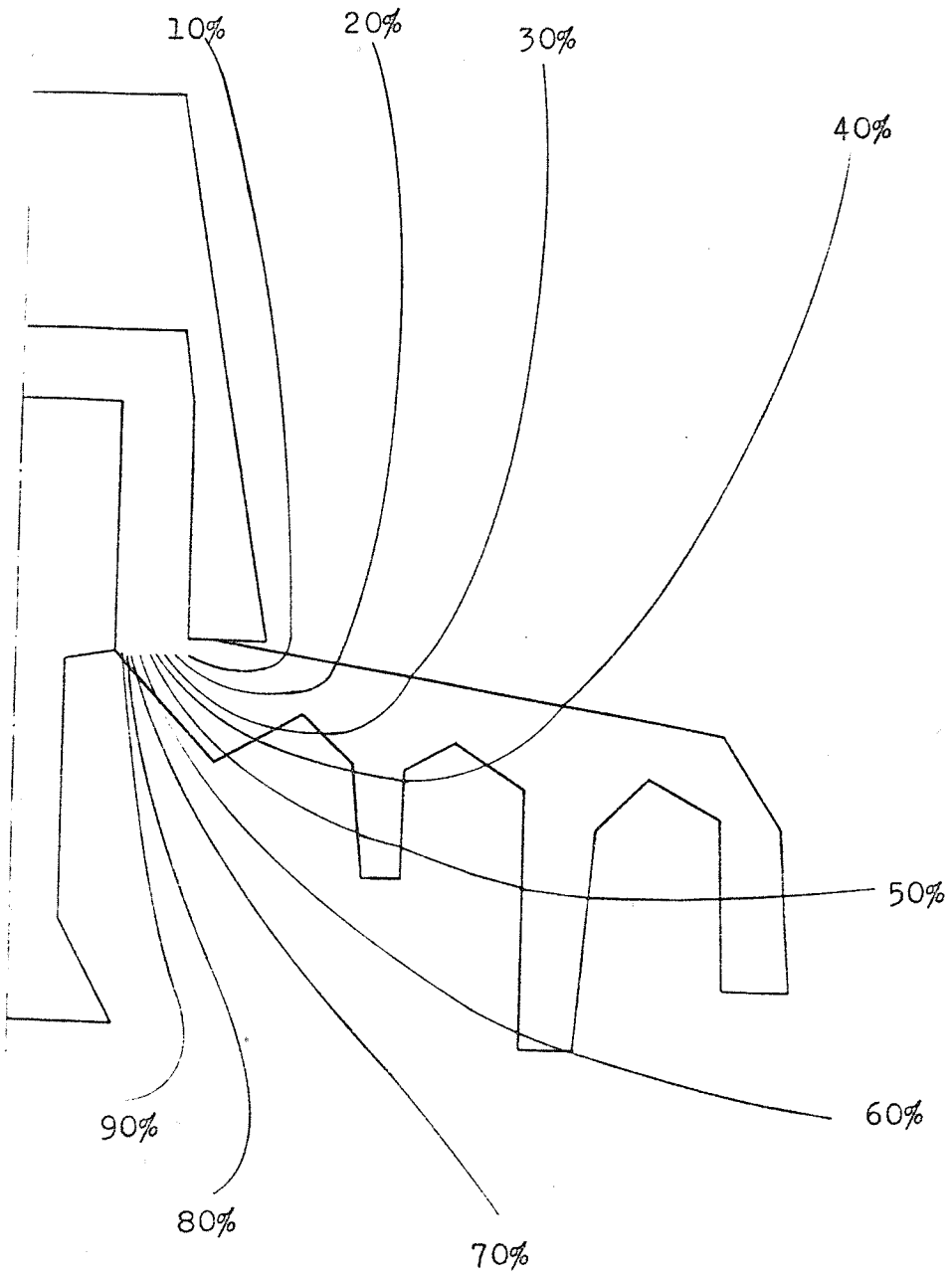

Fig. 4.5- Equipotential Lines For The Simulated Insulator.

- $N1 + 1 \leq m \leq N1 + N2$

- N2 is the total number of subsurfaces across dielectrics interface.

L_{mn} is given by equation (4.16)

$$0 = \sum_{n} L_{mn} Q_{n} \qquad (3.20)$$

where
- n is the number of subsurfaces on each floating electrode with unknown potential.

- $N1 + N2 + 1 \leq m \leq N1 + N2 + N3$

- N3 is the total number of floating electrodes.

- L_{mn} is the surface of each cone frustum.

The problem unknownsare $N = N1 + N2$ surface charge densities plus N3 potential values of the floating electrodes. Due to floating electrodes the matrix of coefficients is not dense as was the case for single insulator problem. The matrix of coefficients is illustrated in Fig. (4.6).

4.7.1 Axisymmetric Insulator Chaim Consisting of 6 Insulator Units

Fig. 4.7 illustrates an insulator chain made of 6 single unit insulators shown in Fig. 4.3. Potential distribution across the chain and equipotential lines were determined, applying the integral equation methods. Insulators number 1 to 5 are approximated with 14 subsurfaces and insulator number 6 is approximated with 15 subsurfaces. WIth the exception of the electrodes at both ends of the string with the potentials of 1 and 0 percent, the rest are floating electrodes with unknown potentials (N3 = 5). The equipotential lines and voltage

distribution across the chain are illustrated in Figs. 4.7 and 4.8. The total computation time is 8.42 seconds, which is the time to solve the matrix equation and checking the accuracy criteria 1 to 4. The maximum potential error on the electrodes is -3.2 percent. The maximum electric field deviation angle is 16.2 degrees and maximum normal displacement error on the dielectrics interface is 6.3 percent. The check points are distributed across the boundary with the density of 5 points per unit length.

4.7.2 Axisymmetric Insulator Chain Consisting of 21 Insulator Units

Generally, as the number of insulator units of the chain increases, two major difficulties arise:

1. The number of surface divisions increase with the number of insulator units. Thus, the number of the elements of the matrix of coefficients increase in proportion to the square of the number of the subsurfaces; the computation time increases in proportion to the cube of the matrix dimension. Furthermore, the matrix elements which must be stored in the computer memory is equal to the square of matrix dimension. Thus, some limitation may arise regarding the computer memory.

2. Practically, increasing the number of surface subdivisions results in the singularity of the coefficients matrix. As the matrix of coefficients approaches singularity the error increase rapidly. Thus, the application of the integral equation method for the field evaluation of long insulator chains requires careful surface approximation.

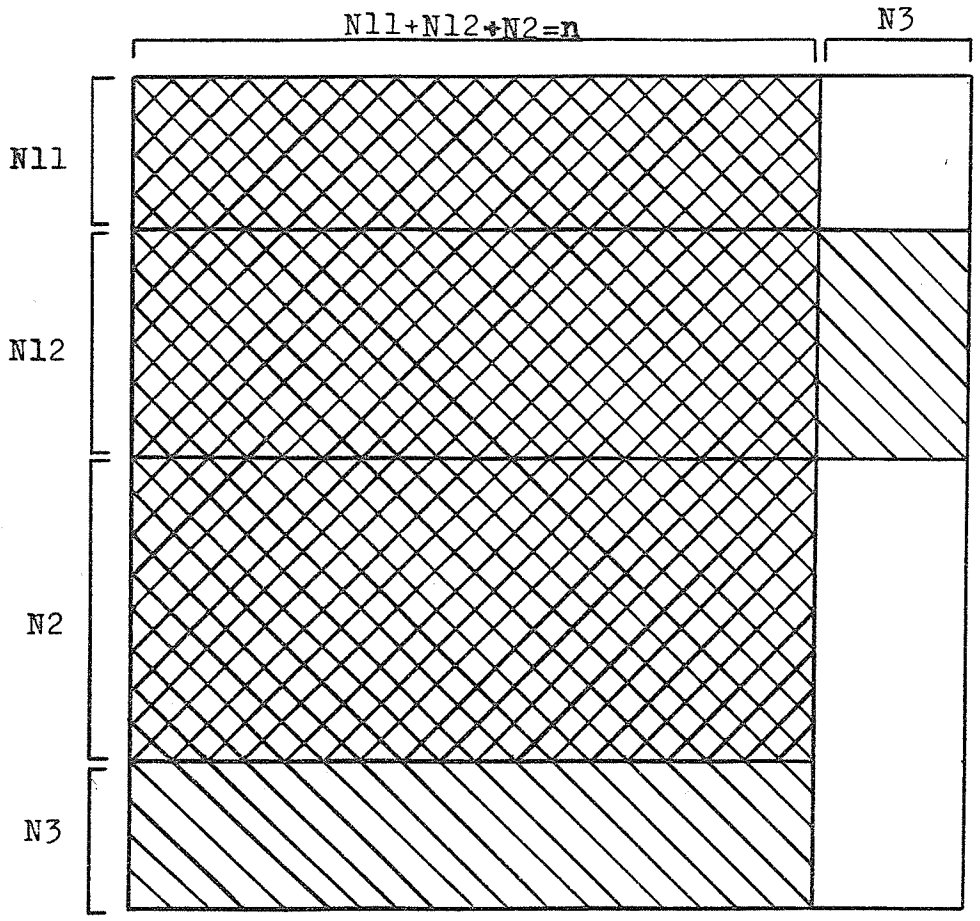

Fig. 4.6- Matrix Of Coefficients.

Dense Part

Sparse Part

Zero Part

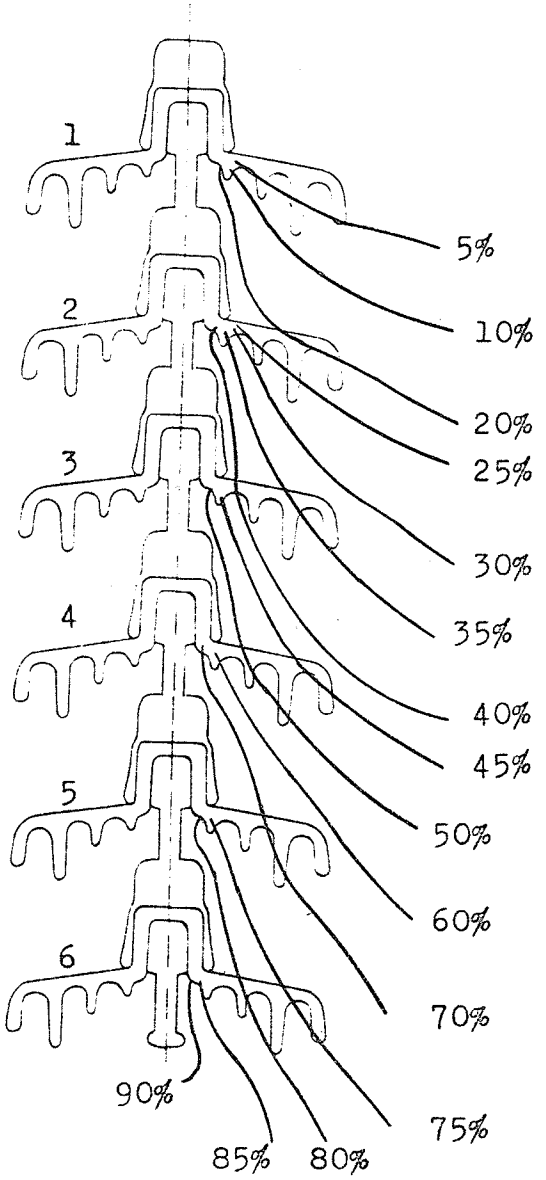

Fig. 4.7- Equipotential Lines For A 6 Units Insulator Chain.

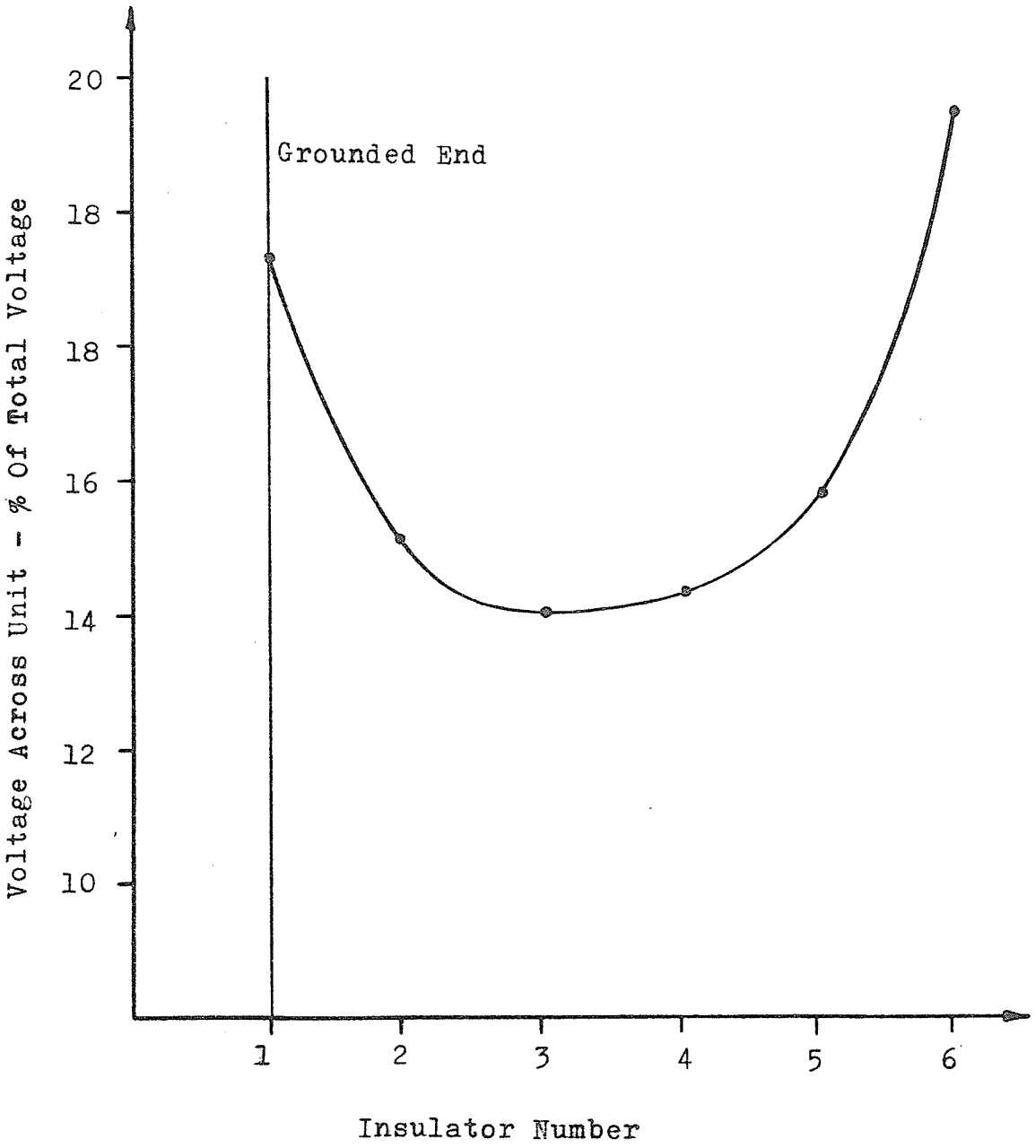

Fig. 4.8- Voltage Distribution Along Insulator Chain.

TABLE 4.1

		Potential error Max. (Percent)	Deviation angle Max. (degree)	Normal $\bar{D}$ error Max. (Percent)
Fig. 3.4a	Cap	3.83	10.72	-
	Pin	2.67	7.01	-
	Dielectric Interface	-	-	3.42
Fig. 3.4b	Cap	2.93	8.00	-
	Pin	2.70	8.36	-
	Dielectric Interface	-	-	3.18

Figure 4.9 shows the insulator chain of a 400 kv DC line which is made of 21 insulator units (Fig. 4.3). To calculate the potential distribution of chain, each insulator unit was approximated with 6 subsurfaces which correspond to 2, 3 and 1 subsurfaces for the cap, glass and the pin, respectively. It was noticed that the effect of polarization charges on the charge distribution which is far enough is negligible: *i.e.*, the effect of polarization charges of insulators 1 to 14 on the charge distribution over insulators 18 to 21 are negligible. This approximation introduces zero bands in the dense part of the coefficients matrix (Fig. 4.6). Thus, the required computer memory can effectively be reduced, also the computation time will be reduced.

The equipotential lines and the voltage distribution across the insulator chain are illustrated in Figs. 4.9 and 4.10. The total computation time is about 39 seconds. Due to the rough surface approximation the potential error and deviation angle are higher compared to the results obtained for the single unit insulator field problem.

If a more accurate the solution at a specific region around a long insulator chain is required the foregoing solution can be employed to determine the potential values of floating electrodes and the charge values of the insulators which are far from the interested region. In the next step the insulators which are closed to the pre-specified region are modelled carefully. Considering the effect of calculated charges the matrix equation of the system can be obtained, which results in more accurate field quantities.

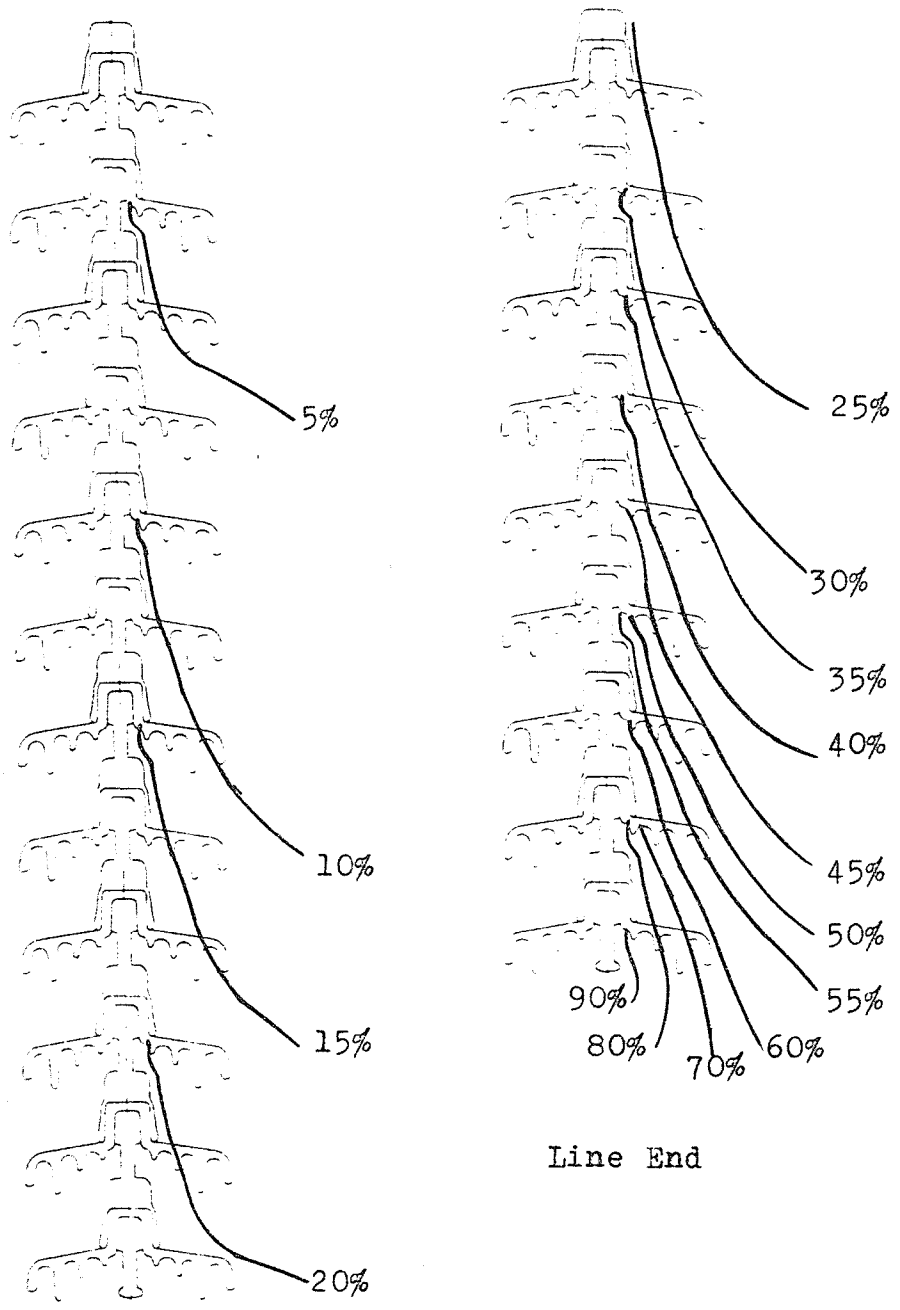

Fig. 4.9- Equipotential Lines For An Insulator Chain Composed Of 21 Units.

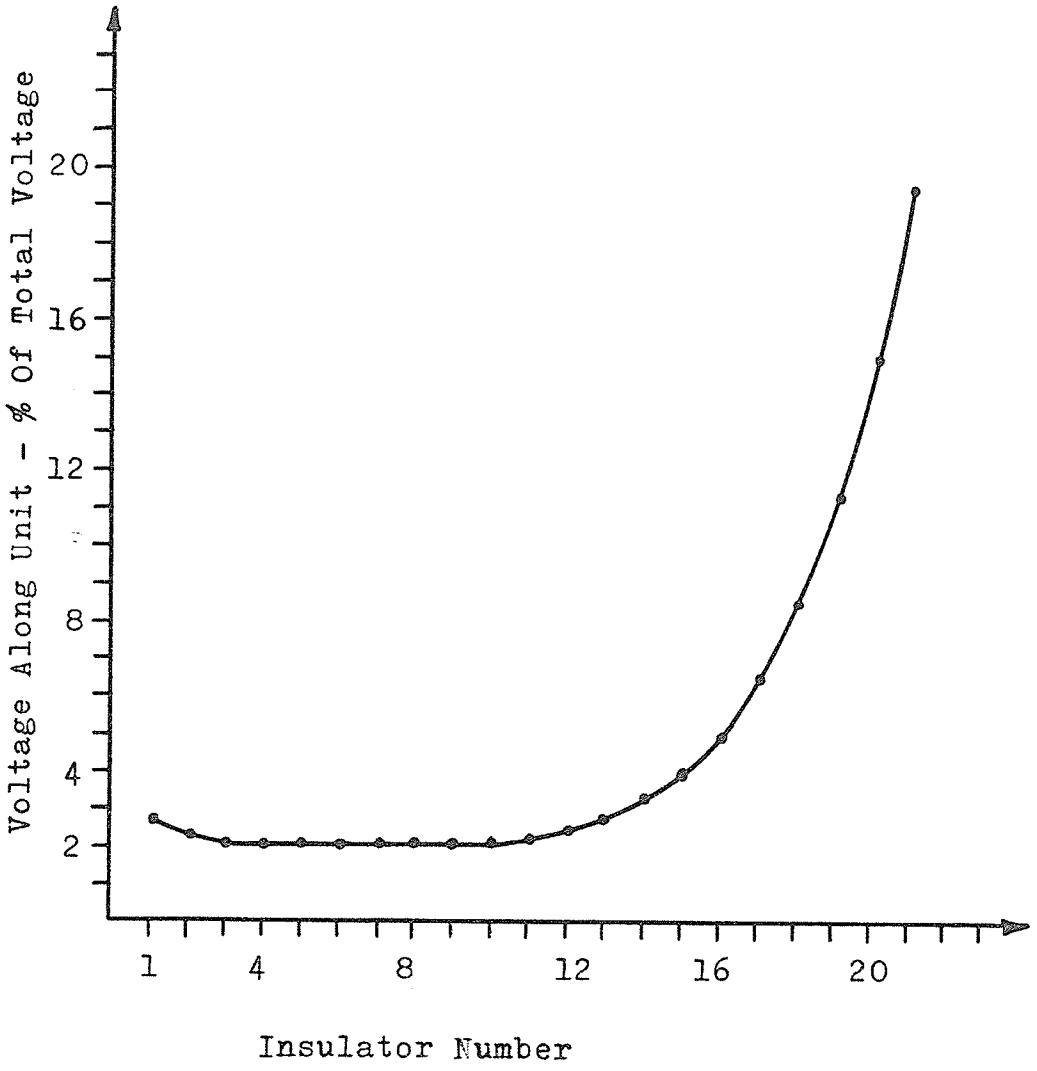

Fig. 4.10- Voltage Distribution Along Insulator Chain Composed Of 21 Units.

CHAPTER V

FIELD CALCULATION OF A NON-AXISYMMETRIC H.V. INSULATOR CHAIN

5.1 Introduction

In this chapter, the integral equation method discussed in Chapters 3 and 4 is developed for the field calculation of a non-axisymmetric H.V. transmission line insulator chain. A constant sectorial surface charge is suggested in order to take into account the non-axisymmetric surface charge distribution. Different methods for considering the effect of conducting bodies around the insulator chain are discussed. Finally a combination of the integral equation method and the charge simulation technique is employed for field computation of the insulator chain, with the effects of tower, cross-arm, line conductors and ground are taken into account. As an example, the insulator chain field problem of a 400 kV D.C. transmission line is solved. The effects of conductors, cross-arm, ground plane, and tower on potential distribution across the insulator chain are discussed.

5.2 Mathematical Model of the Problem

Figure 5.1 shows the front view of a 400 kV D.C. transmission line. Accurate knowledge of the potential and field distribution along the insulator chain requires proper mathematical modelling of the problem, which depends on the geometry. Neglecting the effects of surrounding metallicparts such as line conductors, tower and cross-arm, results in an axi-symmetric field problem, which is much easier to evaluate.

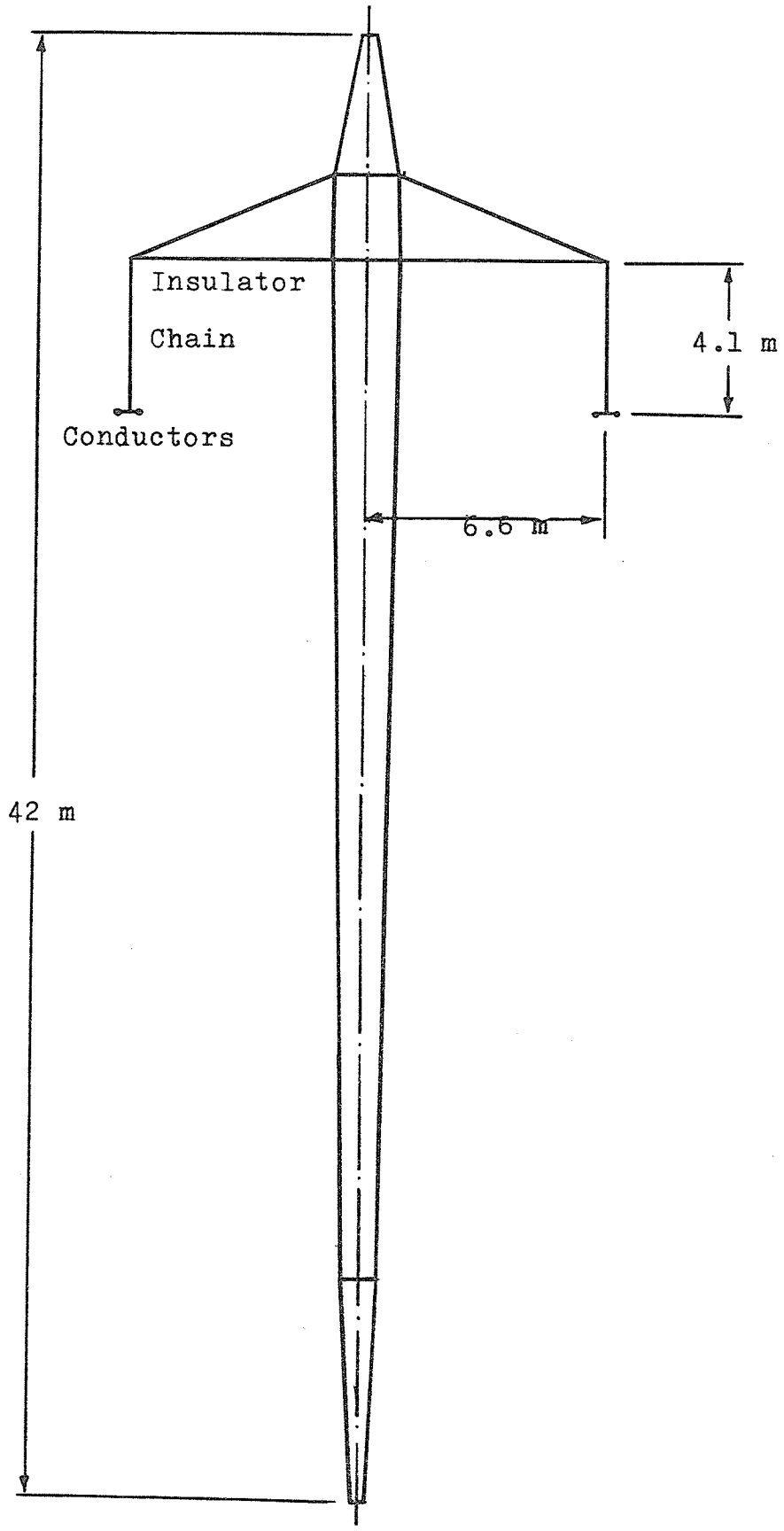

Fig. 5.1- Tower Front View Of A 400 kv HVDC Transmission Line.

However, this evaluation may be in considerable error. Generally, there are three basic difficulties in the mathematical modelling of a non-axi-symmetric insulator chain.

1. Complicated geometry of the problem;
2. Unbounded space inside which calculation must be carried out; and
3. Influence of adjacent conducting bodies with known potential.

The mathematical model must be capable of overcoming these difficulties within the constraints of practical limitations such as computer memory and time, without reducing the accuracy of the results.

The effects of conductors, cross-arm, tower, and ground on the field and potential distribution of the insulator chain, can be taken into account by employing the charge simulation method and/or image principle.

Image Principle: The method of images is useful when it is desired to find the field arising from an object in the vicinity of conductors of a certain simple shape. For the case shown in Fig. 5.2a, boundary condition require that the potential along the grounded plane be zero. This requirement is met if, in the place of conducting surfaces, an equal and opposite image charge is placed at the mirror image position of the object with respect to the ground plane. If the plane potential is other than zero, the value of this constant potential is simply added to the potential expression from the main charge and its image to give the final potential value at any point.

For a charge in the vicinity of the intersection of conducting planes, as q in the region of AOB Fig. 5.2b, the imaging procedure is different. In this case, it is necessary to image the images in turn,

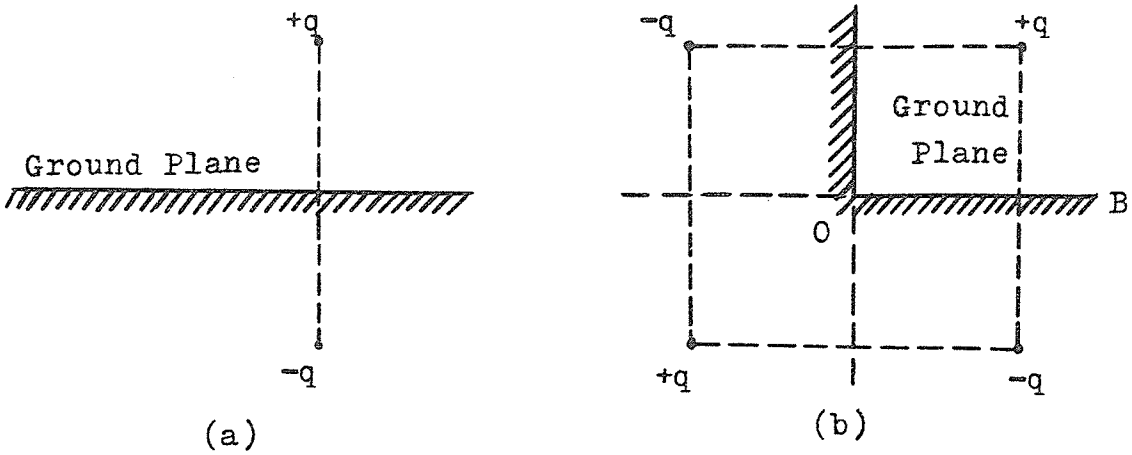

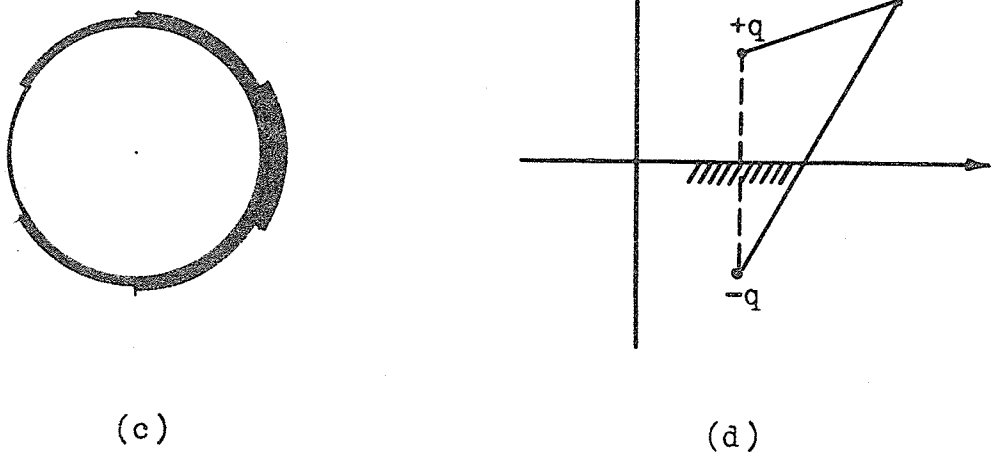

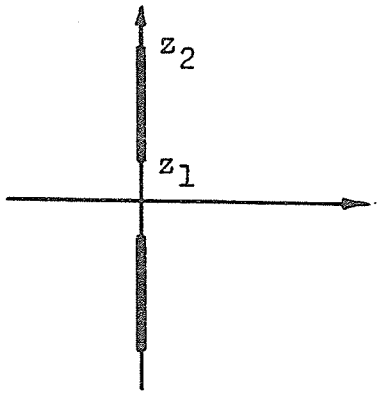

Fig. 5.2- Different Forms Of Charge Approximation For The System Of Insulator Chain , Conductors,Tower,Cross-Arm And Ground.

repeating until further images coincide, or all further images are too far distant from the region to influence the potential. It is possible to satisfy exactly the required conditions with a finite number of images only if the angle AOB is an exact multiple of 360°. Except for some simple geometries such as planes and spheres, one cannot determine the location and strength of the images. It should be mentioned that in some cases this difficulty can be overcome by determining a set of simulated images using an optimization technique[54].

Charge Simulation Method: The charge simulation method can be employed to model the tower, cross-arm and line conductors, with fictitious charges. Depending on the dimensions and the geometry, infinite line charge, finite line charges, point charges, and ring charges, or a combination of these can be used to model each metallic part. The principle of the charge simulation method is described in Chapter II.

For the case under consideration, due to the complexity of the geometry of the ground object (ground plane + tower + cross-arm) direct application of charge simulation method is simpler and used to model the tower, cross-arm and conductors. The effect of the ground plane on the potential distribution is taken into account by means of imaging the charges simulating line conductors, tower, and cross-arm, with respect to ground. The insulator chain is modelled using constant sectorial charge distributions discussed below.

5.3 Mathematical Model of the Insulator Chain

For the case of the non-axisymmetric field problem, the surface of the chain can be approximated with lateral cone frustum subsurfaces, the same as described in Chapter IV for the symmetric case. But, due to

lack of axial symmetry, the charge density over each subsurface can not be constant. The charge distribution over each segment can be expressed as a constant part plus several cosinusoidal (or sinusoidal) harmonics with unknown peak values, q_i, as in Fourier analysis. In this case the charge distribution over each segment is a function of the rotation angle θ and can be given by

$$q(\theta) = \sum_i q_i \cdot \cos(i\theta) \qquad (5.1)$$

where $0 \leq i \leq n$

n is the total number of harmonics

The value of q_i is not calculated by fulfilling the orthogonality condition as is the case for Fourier analysis. The q_i's can be obtained by application of the boundary conditions at the points located on the subsurface of interest. The total number of these contour points is $(n + 1)$, which is equal to the number of unknown charges of each segment.

An alternative is to divide the lateral cone frustum subsurface into sectorial segments. The surface charge distribution over each segment is maintained constant. Therefore, rotational symmetry does not exist. Figure 5.2c illustrates a radial section across a subsurface of the insulator chain which is shown with 6 segmental surface charges. The number of segments can be changed to suit the accuracy required.

In this work, each subsurface is divided into 4 sectors. The integral equationsfor the insulator chain are described by equations (3.20), (4.13) and (4.15). For this problem the coefficients L_{mn} involve incomplete elliptic integrals which can be handled numerically (Appendix 2).

5.4 Mathematical Model of the Conductors

The simulation of the charge distribution on the surface of a conductor by line charges of infinite length is a known principle for the electrostatic field evaluation of circular cylinders. Since the line charge is of infinite length, the quantity to be determined is the charge per unit length q. The effect of the ground plane is considered by the image of the infinite line charge with respect to ground. The potential coefficient of an infinite line charge and its image (Fig. 5.2d) is defined as

$$L = 1/(2 \cdot \pi \cdot \varepsilon) \cdot \ell n[r_2/r_1] \tag{5.2}$$

where $r_2 = [(y + y')^2 + (x - x')^2]^{\frac{1}{2}}$

$r_1 = [(y - y')^2 + (x - x')^2]^{\frac{1}{2}}$

(x,y) is the field point location

(x',y') is the source point location

The electric field vector $\bar{E}$ at point (x,y) is given as

$$\bar{E} = - \nabla\phi \tag{5.3}$$

$$\bar{E} = q/(2 \cdot \pi \cdot \varepsilon) \cdot [(x-x')/r_1 - (x-x')/r_2]\bar{i}$$

$$+ q/(2 \cdot \pi \cdot \varepsilon) \cdot [(y-y')/r_1 - (y-y')/r_2]\bar{j}$$

5.5 Mathematical Model of the Tower and Cross-Arm

The tower and cross-arm, Fig. 5.1, are modelled with 3 and 2 finite line charges, respectively. The effect of ground plane on the potential distribution of thesefinite line charges are taken into account by their image charges with respect to ground. The potential coefficient

and the field component of a finite line charge (Fig. 5.2e) at point (r,z) are given:

$$L = 1/4\pi\varepsilon(z_2 - z_1) \cdot \ln [[(z_2 - z + A) \cdot (z_1 + z + B)]/ [(z_1 - z + C) \cdot (z_2 + z + D)]] \qquad (5.4)$$

$$E_r = q/4\pi\varepsilon(z_2 - z) \cdot [(z_2 - z)/r \cdot A - (z_1 - z)/r \cdot C + (z_1 + z)/r \cdot B - (z_2 + z)/r \cdot D]$$

$$E_z = q/4\pi\varepsilon(z_2 - z_1) \cdot [1/A - 1/C - 1/B + 1/D]$$

where q is the charge density

$$A = [r^2 + (z_2 - z)^2]^{\frac{1}{2}}$$

$$B = [r^2 + (z_1 + z)^2]^{\frac{1}{2}}$$

$$C = [r^2 + (z_1 - z)^2]^{\frac{1}{2}}$$

$$D = [r^2 + (z_2 + z)^2]^{\frac{1}{2}}$$

As mentioned before, the effect of ground on the potential and field distribution of the insulator chain is taken into account, employing image charges of the line conductors, cross-arm, and the tower. Calculation results indicate that for the region in the vicinity of the chain the effect of ground on the field distribution is not significant. However, this effect at region close to ground is quite noticeable.

5.6 Discussion of Results

Curve (a) in Fig. 5.3 illustrates the potential distribution along the chain when the effect of tower, cross-arm and conductors are taken into account. Comparison of this curve in Fig. 5.3 with Fig. 4.10 indicates that due to the environmental effects, the potential distribution across the insulator chain is altered. This effect is especially more significant for the insulators which are close to the line conductors. Curve (b) in Fig. 5.3 shows the potential distribution when the effect of transmission line conductor is neglected. Comparison of curves (a) and (b) indicates that as the result of the conductor surface charge distribution, the voltage distribution non-uniformity increases. Curve (c) in Fig. 5.3 represents the voltage distribution along the chain, when the cross-arm effect is neglected. Comparison of curve "c" with curve "a" shows that the presence of cross-arm increases the voltage supported by the insulators at the line end, and decreases the voltage supported by the insulator at the ground end. The line conductors have more influence on the voltage supported by the line end units than the cross-arm. Equipotential lines for this insulator chain in the plane that passes through the axes of insulator chain and tower are shown in Fig.5.4 .

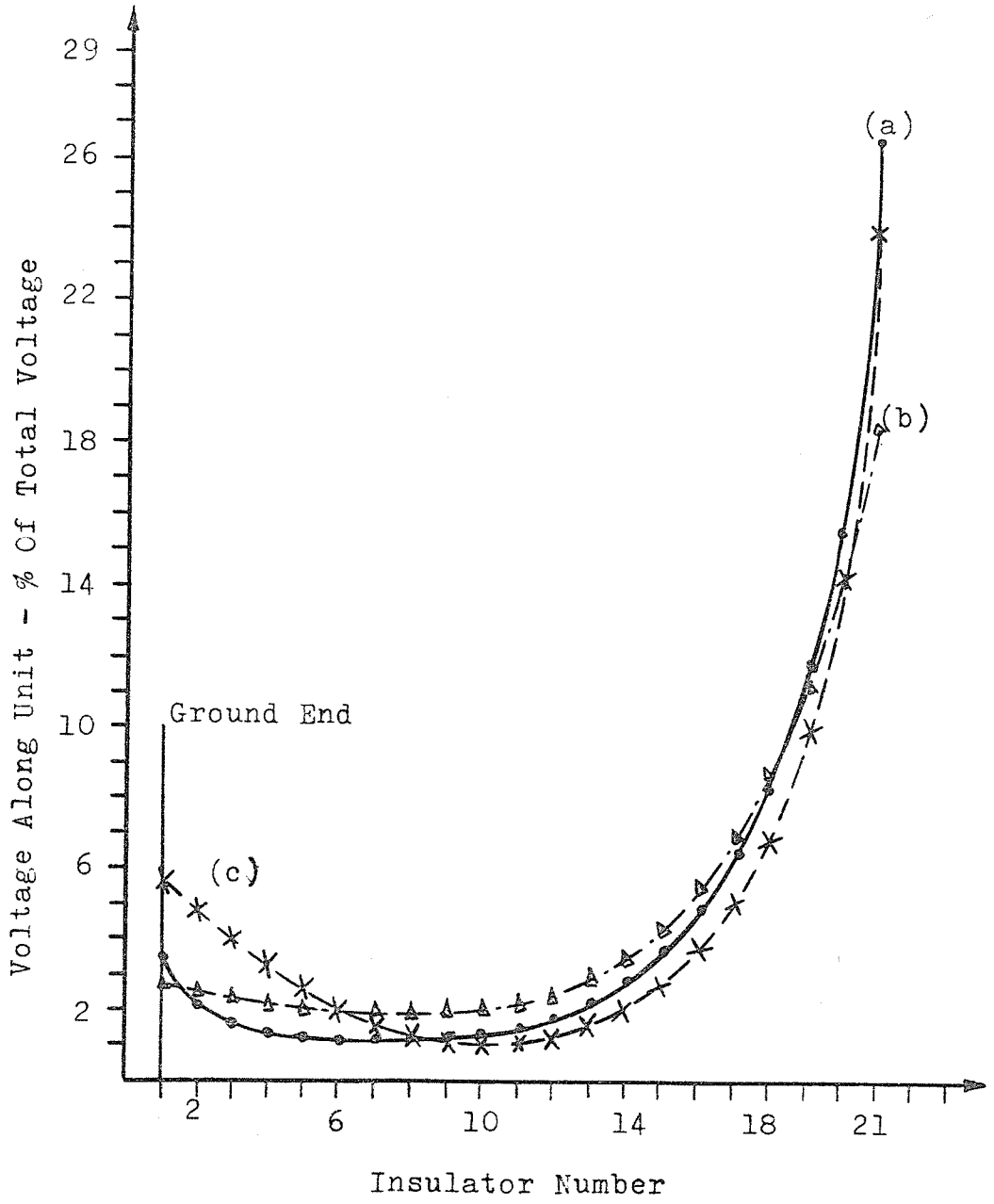

Fig. 5.3 - Voltage Distribution Along Insulator Chain.

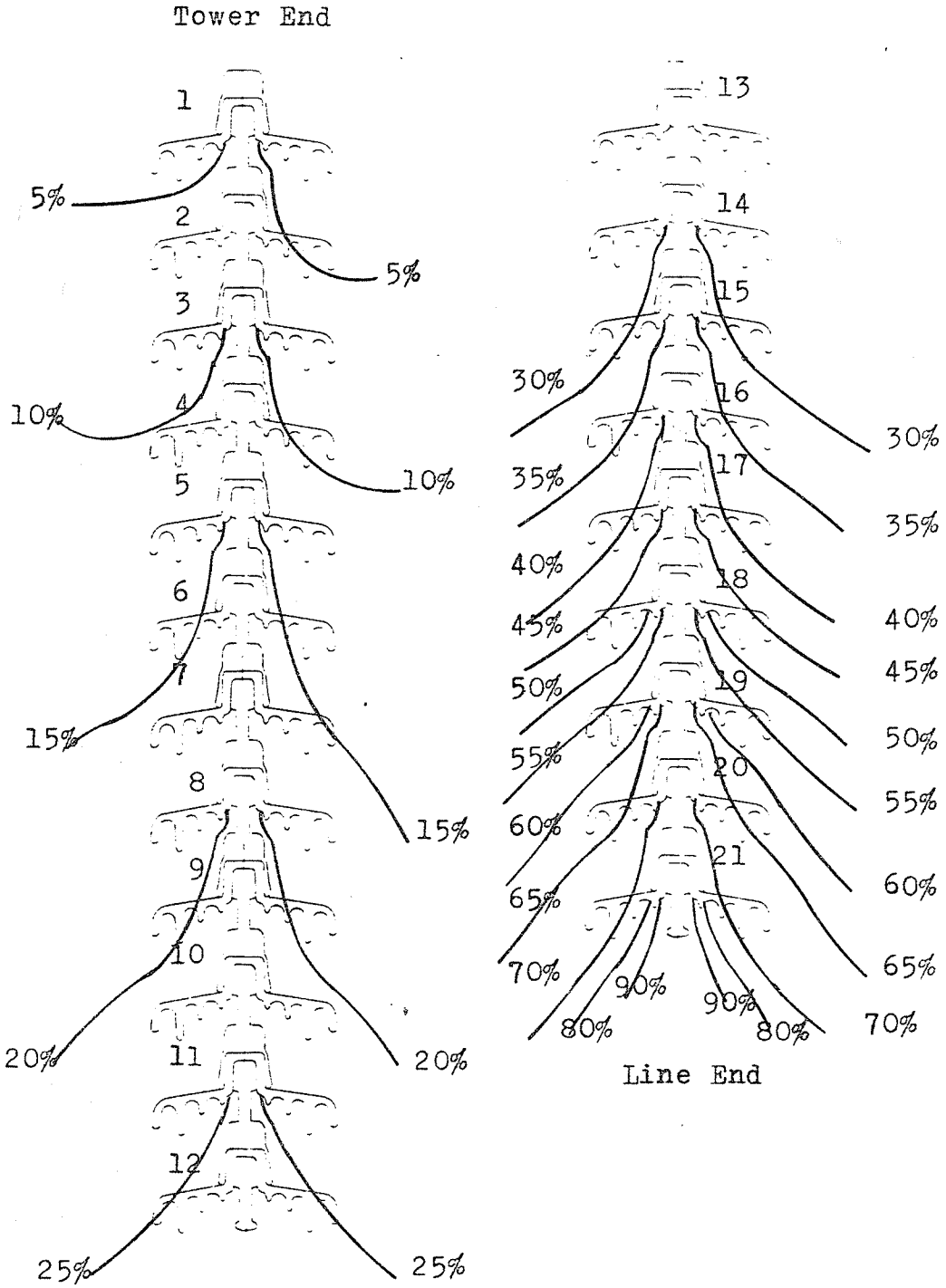

Fig.5.4 - Equipotential Lines For An Insulator Chain Composed Of 21 Units , In The Cross-arm And Chain Plane.

CHAPTER VI

CONCLUSIONS

6.1 The Numerical Method

1. In the present work, it is shown that the integral equation method has several advantages over other available numerical methods for the electrostatic field evaluation of HV insulator chains. The integral equation method reduces the number of linear algebraic equations compared to other techniques. This results in a smaller computation time. Also, this method allows the field calculation at any desired point without extra programming effort.

2. Three coupled integral equations are described which in principle can be used to solve three-dimensional electrostatic field problems. In general form, the field domain may be composed of conductor-dielectric boundaries with known and unknown potential values and dielectric-dielectric boundaries.

3. A combination of the integral equation method and the charge simulation technique is described which can be used to solve the electrostatic field problem of un-conventional and complicated geometries.

4. The programs are developed in general form and can be employed to solve any electrostatic field problem with the boundary conditions described for a H.V. transmission line insulator chain in multi-dielectric media.

6.2 Insulator Chains

An integral equation method has been used to solve the three-dimensional H.V. insulator chain field problem. Such an approach to solve a problem of this nature has been reported in the literature this far. The mathematical model of the insulator chain, the numerical method and the developed program can be applied to compute the field and potential distribution of any H.V. transmission line insulator chain. Furthermore, the chain is considered to be in its real situation, *i.e.*, the influence of all conducting bodies in the vicinity of the chain as well as the ground effect are taken into account.

The described method can be used to solve the problems related to the design of insulator unit and chain. Also, it is possible to assess the effect of the design parameters of the insulator chain on the potential and field distribution, *i.e.*, type of insulator unit and inter-unit spacing.

It is shown that the tower has not a considerable effect on potential distribution along the insulator chain. The cross-arm effect on the voltage of the line end insulators is noticeable. The conductors have the most significant effect on potential distribution along the insulator chain. The presence of the line conductors introduces about 6% increase on the voltage of line end insulator. In summary, one can obtain a realistic potential distribution along a H.V.D.C. transmission line insulator chain, considering the effect of conductors and cross-arm on the potential distribution.

6.3 Suggestion for Further Work

Matrices obtained from discretization of the integral equation are dense. Consequently, in the computation of the field quantities, one can easily run into problems of insufficient computer memory as well as of a large computation time. It is possible to overcome this difficulty by introducing a sort of a block structure to the original matrix. This is accomplished by an artifical division of given domain into several subdomains, which is called artificial partitioning technique.

REFERENCES

[1] K.J. Binns and P.J. Lawrenson, Analysis and Computation of Electric Field Problems, Pergamon Press, Oxford, 1962, pp. 241-287.

[2] R.H. Galloway, "Calculation of electric field by digital computer," IEE Proc., Vol. 114, pp. 824-829, 1967.

[3] H.M. Ryan, "Computation of electric field distribution in high voltage equipment," IEEE Trans. on Electrical Insulation, Vol. EI-6, pp. 148-154, 1971.

[4] C.M. Dorney, "Finite difference method for determining capacitance relationship among arbitrary shape conductors," IEEE PAS, Vol. 90, pp. 876-881, 1971.

[5] P.A. Einstein, "Off axial mapping with boundary compensation in axisymmetric problems," IEE Proc., Vol. 123, pp. 472-476, 1976.

[6] P.A. Einstein, "Boundary compensation in the mapping of Laplace fields using a computer program," IEE Proc., Vol. 120, pp. 1048-1054, 1973.

[7] P.A. Einstein, "Finite mapping using a computer, compensation for infinite space," IEE Proc., Vol. 121, pp. 149-153, 1974.

[8] J.T. Storey, "General digital computer program for determination of three-dimensional electrostatic axially symmetric fields," IEE Proc., Vol. 114, pp. 1551-1555, 1967.

[9] M.J. Billings, "Consideration of the effect of pollution on the potential distribution of insulator system," IEE Proc., Vol. 115, pp. 1661-1666, 1968.

[10] G. Motinari, "Experimental results and computer simulation of electric field around insulating structure under AC and DC conditions," ISM, Milan, 1979, #12.17.

[11] P.A. Einstein, "Field mapping using a computer, simple procedures across machinery boundary," IEE Proc., Vol. 122, pp. 330-332, 1975.

[12] P.A. Einstein, "Field mapping using a computer, assessment of some computing errors and further improvement in accuracy," IEE Proc., 122, pp. 327-329, 1975.

[13] J.A. Cermack, "Boundary relaxation analysis of rotationally symmetric electric field problems," IEEE PAS, Vol. 89, pp. 925-932, 1970.

[14] J.A. Cermack, "Solution of 2-dimensional field problems by boundary relaxation," IEE Proc., Vol. 115, pp. 1341-1348, 1968.

[15] Z. Hazander, "Numerical field calculation of insulator chains for high voltage transmission lines," ISM, Millan, 1979, #12.08.

[16] O.W. Anderson, "Finite element solution of complex potential electric fields," IEEE PAS, Vol. 36, pp. 925-932, 1970.

[17] J.M. Janiszewski, "Improved finite element method for static electro-magnetic field mapping," ISM, Milan, 1979 #11.10.

[18] O.C. Zienkiewicz, "Numerical solution of 3-dimensional field problems," IEE Proc., Vol. 115, pp. 367-369, 1968.

[19] K. Itaka, "New finite element field calculation technique in which continuity of electric flux is satisfied," IEEE PAS, Vol. 99, pp. 2102-2111, 1980.

[20] K.H. Huebner, The finite element method for engineers, John Wiley & Sons, Toronto, 1975.

[21] P. Silvester, "High order polynomial triangular finite element for potential problems," Int. J. Eng. Sci., Vol. 7, No. 8, pp. 849-861,

[22] O.W. Anderson, "Laplacian electrostatic field calculation by finite element with automatic grid generation," IEEE PAS, Vol. 92, pp. 1485-1492, 1973.

[23] H. Okuto, "Calculation error and field discretization on finite element method," ISM, Milan, 1979, #11.01.

[24] P. Silvester, "Exterior finite element for 2-dimensional field problems with open boundaries," IEE Proc., Vol. 124, pp. 1267-1270, 1977.

[25] R.W. Thatcher, "On the finite element method for unbounded regions," SIAM Journal of Numerical Analysis, Vol. 15, pp. 466-477,

[26] O.C. Zienkiewicz, "The coupling of finite element method and boundary solution procedures," Int. Journal Numer. Method Eng., 1977, pp. 355-375.

[27] M. Steinbigler, "Combined application of finite element method and charge simulation method for the computation of electric field," ISM, Milan, 1979, #11.11.

[28] M. Ikabo, "Combination method for electric field calculation," ISH, Milan, 1979, #11.13.

[29] J.H. Pickles, "Monte Carlo field calculation," IEE Proc., Vol. 124, pp. 1271-1276, 1977.

[30] M.D.R. Beasley, "Comparitive study of three methods for computing electric fields," IEE Proc., Vol. 126, pp. 126-134, 1979.

[31] Hayi-Sheikh, "The solution of heat conduction problems by probability method," Trans. ASMEC, J. Heat Transfer, C-89, pp. 121-131, 1967.

[32] W.M. Rohsenow, Heat, Mass and Momentum Transfer, Prentice-Hall, Englewood Cliffs, New Jersey, 1961, pp. 94-96.

[33] E.L. Coffey, "Hybrid computer solution of electromagnetic scattering problems," IEEE APS International Symposium Digest, 1976, pp. 82-85.

[34] J.R. Mantz, "Computation of rotationally Laplacian potential," IEE Proc., Vol. 117, pp. 850-852, 1970.

[35] R.F. Harrington, "Computation of Laplacian potential by an equivalent source method," IEE Proc., Vol. 116, pp. 1715-1720, 1969.

[36] J. Daffe, "An integral equation technique for solving electrostatic problems in conducting and dielectric materials," IEEE PAS, Vol. 98, pp. 1609-1616, 1979.

[37] R.F. Harrington, Field Computation by Moment Method, MacMillan, New York, 1968.

[38] A. Jennings, Matrix Computation for Engineers and Scientists, New York, John Wiley, 1977, pp. 145-178.

[39] A. Marten, "A partition technique for the solution of potential flow problems by integral equation method," Journal of Computational Physics, Vol. 27, pp. 71-84, 1978.

[40] H. Singer, "A charge simulation method for the calculation of high voltage fields," IEEE Pas, Vol. 93, pp. 1660-1668, 1974.

[41] H. Parekh, "Computation of electric field and potential around stranded conductors by analytical method and comparison with charge simulation method," IEE Proc., Vol. 122, pp. 547-550, 1975.

[42] M.S. Abou-Seada, "Digital computer calculation of electric potential and field of a rod gap," IEEE PAS, Vol. 122, pp. 813-820, 1968.

[43] D. Utmischi, "Charge substitution method for the three-dimensional high voltage fields," ISH, Milan, 1979, #11.01.

[44] S. Koto, "An estimation method for the electric field error of the charge simulation method," ISH, Milan, 1979, #11.09.

[45] H. Parekh, "Computation of potential and field of a stranded twin-bundle conductor above ground," IEEE Winter Meeting, 1974.

[46] E.U. Landers, "Computation of asymmetric, three-dimensional fields with any input conditions," ISH, Milan, 1979, #11.02.

[47] M.S. Abou-Seada, "Calculation of potential gradient of twin cylinderical bipolar conductors with various geometrical parameters," IEEE PAS, Vol. 90, pp. 1822-1829, 1971.

[48] A. Yializis, "An optimized charge simulation method for the calculation of high voltage fields," IEEE PAS, Vol. 97, pp. 2434-2440, 1978.

[49] A. Nicoluide, "A method of distributed charges for solving problems of electromagnetic field in non-homogeneous media," IEEE, PAS, Winter Meeting 1978, F78-178-6.

[50] O.D. Kellogg, Foundation of Potential Theory, Berlin, Springer, 1929, pp. 164.

[51] P.F. Byrd and M.D. Friedman, Handbook of Elliptic Integrals for Engineers and Physicists, Berlin, Springer, 1954.

[52] R.F. Harrington, "Matrix method for field problems," IEEE PAS, pp. 136-149, 1967.

[53] E. Kreyszing, Advanced Engineering Mathematics, John Wiley and Sons, Toronto, 1979, pp. 784-790.

[54] V.L. Chow, "Static field computation by the method of optimized simulated images," IEE Proc., Vol. 126, pp. 123-125, 1979.

[55] J.A.Stratton,'Electromagnetic Theory" New York, McGrow -Hill, 1941,P.165

APPENDIX 1

Green's Theorem

Let V be a closed region bounded by a regular surface S, and ϕ and ψ be two scalar functions of position which together with their first and second derivatives are continuous throughout V and on S. The divergence theorem applied to the vector $\psi\nabla\phi$ gives

$$\int_V \nabla \cdot (\psi\nabla\phi)\, dv = \int_S (\psi\nabla\phi) \cdot \bar{n} \cdot ds \qquad (A.1)$$

where $\bar{n}$ is the normal unit vector. Expanding the divergence, and where $\partial\phi/\partial n$ is the derivative in the direction of the positive normal, we obtain what is called as Green's first identity

$$\int_V \nabla\psi \cdot \nabla\phi\, dv + \int_V \psi\nabla^2\phi\, dv = \int_S \psi \frac{\partial\phi}{\partial n}\, ds \qquad (A.2)$$

If in particular case $\psi = \phi$ and ϕ be a solution of Laplace's equation

$$\int_V (\nabla\phi)^2\, dv = \int_S \psi(\partial\phi/\partial n) \cdot ds$$

If the rules of the function ϕ and ψ are changed, *i.e.*, the divergence theorem is applied to $\phi\nabla\psi$

$$\int_V \nabla\phi \cdot \nabla\psi \cdot dv + \int_V \phi\nabla^2\psi\, dv = \int_S \phi \frac{\partial\psi}{\partial n}\, ds \qquad (A.3)$$

Subtracting 3 from 2 a relation between a volume integral and a surface integral is obtained

$$\int_V (\psi\nabla^2\phi - \phi\nabla^2\psi)dv = \int_S (\psi \frac{\partial\phi}{\partial n} - \phi \frac{\partial\psi}{\partial n})ds$$

known as Green's second identity or Green's theorem.

APPENDIX 2

1. $$\int_0^{2\pi} d\theta'/[(r - r'\cos\theta')^2 + (r'\sin\theta')^2 + (z - z')^2]^{\frac{1}{2}}$$

$$= [2/[(r + r')^2 + (z - z')^2]^{\frac{1}{2}}] \int_{-\pi/2}^{+\pi/2} d\phi/[1 - S^2 \cdot \mathrm{Sin}^2\phi]^{\frac{1}{2}}$$

where $S^2 = 4rr'/[(r + r')^2 + (z - z')^2] \leq 1$ and $\theta' = 2\phi$

$$= [4/[(r + r')^2 + (z - z')^2]^{\frac{1}{2}}] \int_0^{\pi/2} d\phi/[1 - S^2 \cdot \mathrm{Sin}^2\phi]^{\frac{1}{2}}$$

$$= [4/[(r + r')^2 + (z - z')^2]^{\frac{1}{2}}] \cdot K(s)$$

where $$K(s) = \int_0^{\pi/2} d\phi/[1 - S^2 \cdot \mathrm{Sin}^2\phi]^{\frac{1}{2}}$$

2. Expansion of K(s) and E(s) in series:

$$K(s) = (\pi/2) \cdot [1 + (1/2)^2 S^2 + (3/2.4)^2 S^4 + (3.5/2.4.6)^2 S^6 \ldots.]$$

$$E(s) = (\pi/2) \cdot [1 - (1/2)^2 S^2 - (3/2.4)^2 \cdot (S^4/3) - (3.5/2.4.6)^2 \cdot (S^6/5) \ldots]$$

3. Polynomial approximation of K(s) and E(s)

$$K(s) = [a_0 + a_1 (1 - s^2) + a_2 (1 - s^2)^2] + [b_0 + b_1 (1 - s^2) + b_2 (1 - s^2)^2] \ln (1/(1 - s^2)) + (s)$$

where $a_0 = 1.3862944$ $\quad b_0 = 0.5$

$a_1 = 0.1119723$ $\quad b_1 = 0.1213478$

$a_2 = 0.0725296$ $\quad b_2 = 0.0288729$

$$|\varepsilon(s)| \leq 3 \times 10^{-5}$$

$$E(s) = [1 + a_1 (1 - s^2) + a_2 (1 - s^2)^2] + [(b_1 (1 - s^2) + b_2(1 - s^2)^2] \cdot \ell n (1/(1 - s^2)) + \varepsilon(s)$$

where $a_1 = 0.4630151$ $\quad b_1 = 0.2452727$

$a_2 = 0.1077812$ $\quad b_2 = 0.0412496$

$$|\varepsilon(s)| \leq 4 \times 10^{-5}$$

4. Series expansion of incomplete elliptic integrals of the first and the second kind

$$K(\phi, s) = \sum_m \binom{-\frac{1}{2}}{m} (-S^2)^m (t_{2m}(\phi))$$

$$K(\phi, s) = \sum_m \binom{\frac{1}{2}}{m} (-S^2)^m (t_{2m}(\phi))$$

where $0 \leq m \leq \infty$

$0 \leq \phi \leq \pi/2$

$0 \leq S^2 \leq 1$

$t_0(\phi) = \phi$

$t_2(\phi) = \frac{1}{2} (\phi - \text{Sin}\phi \ \text{Cos}\phi)$

$t_4(\phi) = \frac{1}{8} (3\phi - \text{Sin}\phi \ \text{Cos}\phi \ (3 + 2\text{Sin}^2\phi))$

$t_{2m}(\phi) = \frac{2m-1}{2m} t_{2(m-1)}(\phi) - \frac{1}{2m} \text{Sin}^{2m-1}\phi \ \cos\phi$